Preparation of biodegradable polymer composites with flexibility for tissue regeneration

組織再生を目的とした柔軟性を有する生分解性ポリマー複合材料の調製

Pin Zhou

March　2018

Nagoya Institute of Technology

Contents

Chapter I Introduction

1 Demands for tissue regeneration and their treatments with biomaterials

Disease and injury lead to damage, degenerate or loss of human tissues. There are enormous demands each year for various biomedical implants to repair diseased or lost tissues in worldwide. [1] Tissue transplantation is a medical procedure to replace a damaged or missing tissue. Tissues include soft tissues such as skin, tendons, ligaments, fascia, fibrous tissue, muscles, nerves and blood vessels; [2] and hard tissues such as bones, tooth enamel, dentin and cementum. [3]

Conventional tissue replacements, which including autografts, allografts and xenograft, have a variety of problems that cannot satisfy diverse demands for clinical application. [4–6] Currently, autografts remain the primary solution of many clinicians for the repair of dental, craniofacial and orthopaedic bony critical-sized defects. However, autografts require a painful secondary surgery site which increases the risk of patient pain and infection. [7–9] The use of allografts eliminates the need to resect tissue from a secondary location in the body and also does not carry the same risk of disease transmission. [10–11] The technological advances of xenograft materials are more recent and extensive clinical trials are still required due to the many obstacles arising from the interspecific immunologic barriers. [12–13]

Each year, nearly 1 million allografts are transplanted in the U.S. alone. The high incidence of injuries by physical impacts and high percentage of aged population makes the demand of allograft transplantation in Japan increased greatly every year. [14] Soft tissue allografts are substitute tissues that are used to reconstruct deficient ligaments, spinal surgery, torn menisci, and osteochondral defects during knee surgery.

According to Transparency Market Research (TMR) study in 2017, the demand in the global soft tissue allografts market will swell at a healthy compound annual growth rate of 6.3% during the forecast period of 2017 to 2025. The report estimates the market for soft tissue allografts, across the world, to be worth 6.2 billion US dollars by the end of 2025, substantially up from its evaluated valuation of 3.6 billion US dollars in 2016. In order to meet this huge demands, a variety of materials have been developed to mimic specific cell and tissue niches due to the diversity of mechanical and biochemical properties of native human tissue. [15] Biomaterials emerged under this situation and already have applications in tissue regenerative.

Biomaterials is an interdisciplinary field encompasses elements of medicine, biology, chemistry, tissue engineering and materials science. They are designed and expected to restore or augment the physiological function of diseased or damaged tissues via tissue replacement, such as permanent hip replacements; or regeneration. Biomaterials can be obtained from synthesis methods in the laboratory using variety of chemical approaches by utilizing metallic components, polymers, ceramics and/or composite materials. Synthetic biomaterials do not suffer from risks of low supply or high cost associated with autografts and allografts nor do these materials suffer from inconsistency that occurs because of variability in donor bone quality. [16] The biocompatibility, multifunctionality, and physiochemical properties are essential characteristics for biomaterials, because when they incorporate with living cells, integrated systems biology behavioural mimicry can be accomplished. When biomaterials are implanted in human body, cells of the innate immune system are the first to respond to the implantation of a biomaterial in vascularized tissue. Following blood biomaterial contact, a layer of protein immediately adsorbs onto the biomaterial

surface, resulting in the formation of a blood clot; which is rich in growth factors, cytokines and chemoattractants capable of recruiting cells of the innate immune system to the injury site. [17]

2 Therapeutically relevant aspects in biomaterials for tissue regeneration

Tissue regeneration is a part of complex dynamic event that involves many molecules and cells. After implant material implantation, the therapeutic actions should thus be harmonized with the biological events and even facilitate a better healing process. Therapeutic actions include reducing tissue rejection and inflammation, homing progenitor and stem cells, stimulating angiogenesis, improving cellular activity. [18] In order to achieve these biological processes, some key actions need special consideration in designing biomaterials. For example, angiogenesis is critically important because the blood vessels work as the transport of oxygen and nutrients, as well as the metabolic waste. In bone regeneration, especially for large defects, blood vessels must enter the defect, otherwise any new bone will die. For continuous ingrowth of bone tissue, interconnected porosity is important: a minimum pore size between 100 and 150 μm is needed for bone formation; however, enhanced bone formation and vascularization are reported for scaffolds with pore sizes larger than 300 μm. [19–22] In order to produce porous biomaterials, methods such as sol-gel process, particulate-leaching techniques, phase separation, electrospinning and 3D printing, showing effectivity in tuning the porous structure. [23–28] In bone tissue formation, osteogenic differentiation is crucial to obtain specified functional cell from multipotent stem cells. Many physical, chemical, physico-chemical and biological factors have been

implicated in osteogenic stimulation. [29–30] Along with biochemical growth factors, physical and chemical factors are implicated as inducers of stem cell differentiation. Chemical factors include biological ions, which play essential roles in regulating cellular functions, have be widely studied by many research groups. [31–33]

Inorganic ions of calcium (Ca), zinc (Zn), magnesium (Mg), strontium (Sr), silver (Ag), silicon (Si) and cobalt (Co) have shown beneficial effects on bone biological processes including cell mitosis, osteogenesis, angiogenesis or antibacterial properties. [18, 34] Phosphate-based or silica-based bioactive glasses can incorporate those relevant ions within the random networks. [35–36] Different ions can be structured during the thermal (sintering or quenching) processes in preparation processing. As a result, it is possible to control the different levels of these ions release amount. However, the exact mechanism of interaction between the ionic dissolution products from bioactive glasses and human cells are not fully understood, thus many works specifically investigate the effect of the dissolution behavior to osteogenesis angiogenesis and antibacterial activity.

Besides inorganic ions, biochemical growth factors also play an important role in the design of biomaterials for tissue regeneration. [37–38] For instance, tumor necrosis factor α (TNF-α), which can promote osteoblast differentiation and inhibit osteoblast activity. [39] Vascular endothelial growth factor (VEGF), fibroblast growth factor (FGF) and platelet-derived growth factor (PDGF) are widely used to stimulate angiogenic growth. [40]

3 Biodegradable polymer composites for tissue regeneration

Polymer composites employ organic polymer matrix as carrier materials to bear drug, protein or some kinds of inorganic materials. [41–46] The polymer matrix could able to promote the properties of the composite materials such as impact resistance, stability, structural integrity, mechanical flexibility, controlling release, moulding and hydrophilia. Some of promising inorganic biomaterials for application in bone tissue engineering include bioceramics such as hydroxyapatite (HA), octacalcium phosphate (OCP), β-tricalcium phosphate (β-TCP), bioactive glasses and their related composite materials combining inorganic materials with polymers. However, since these inorganic materials are often difficult to process into highly porous structures and are mechanically brittle, composite with polymer matrix could combine to improve their bioactivity and mechanical properties.

For bone tissue healing progresses, it is desirable that the implant materials degrade gradually, and new bone tissues form and start to bear stress at the same time. The non-biodegradable polymers for implantation materials do not display this desired characteristic. To fabricate the ideal implantation materials, biodegradable and bioresorbable linear aliphatic polymers such as poly(glycolic acid) (PGA), poly(D,L-lactic acid) (PDLLA), their copolymer poly(D,L-lactic-*co*-glycolic acid) (PDLLG), poly(L-lactic acid) (PLLA), poly(ε-caprolactone) (PCL), poly(hydroxyl butyrate) (PHB) and poly(propylene fumarate) (PPF), which are frequently used for preparing polymer composite materials for tissue regeneration. [47–48] Numerous researches about inorganic materials/biodegradable polymer composites for tissue regeneration have published. [49–56] Generally speaking, composites can be designed

and produced with specific requirements: by using a wide range of polymeric matrices, reinforcements and processing routes.

In our group, biomaterials with controlled releasabilities of Ca^{2+} and silicate ions consist of siloxane-containing vaterite (SiV) with biodegradable polymeric matrices have been investigated for bone tissue regeneration. [57–61] The vaterite lamellae (5–20 nm in size) build the main structure of SiV with a small amount of amorphous calcium carbonate insert randomly, the γ-aminopropyltriethoxysilane (APTES) distribute enclosed to the main structure. [62] The Si–O–Si bonds form by APTES could be substituted by other stronger-polarity ions. Under this principle, the siloxane-containing vaterite doped with magnesium (MgSiV) was prepared. For the structure of MgSiV, the main structure is principally almost same as that of SiV. While Mg^{2+} ions form Mg–O–Si bonds and aggregate on the surface of calcium carbonate through a deprotonated OH group bonding with Ca^{2+} ions during processing. [63–64]

The Ca^{2+} ion is the most widely studied for bone formation, which mediates multiple cellular responses, including cell proliferation and osteogenesis. [65] Silicate ion also plays a key role in bone growth and has shown excellent *in vitro* and *in vitro* osteogenic potential. [66–67] Except for healing bone, Ca^{2+} and silicate ions are reported to play a central role in wound healing. [68–70] Mg^{2+} ion has been reported to stimulate cellular activity, especially the adhesion of osteoblasts. [71] By combining these therapeutic ions to SiV or SiV-derivative materials (MgSiV), it is meaningful to investigate a series of biomaterials by implementation of SiV.

4 Aim of this thesis

The objective of this thesis is to prepare bioactive composites consisting inorganic materials, SiV or SiV-derivative materials (MgSiV) and biodegradable materials to design flexible biomaterials for tissue regeneration. The ions-release abilities of MgSiV/biodegradable polymers, which were expected to tailor by applying different polymer matrice, were investigated first. Then coaxial electrospinning was implemented to obtain the biocomposites fibrous materials with flexibility and effective ion-release ability for application in tissue regeneration.

In chapter II, the dissolution behavior of MgSiV, embedded in three kinds of biodegradable polymers in Tris buffer solutions (TBS) were examined to find an effective ion releasing system. PLLA and PDLLG (lactide : glycolide = 75 : 25 or 50 : 50; denoted as PDLLG75 or PDLLG50, respectively) were chosen as the matrix polymers. The variety of surface morphologies, ions releasing behaviours, morphologies of cross-section surface and pH values of the immersed solution were traced to evaluate the effect of polymer matrices to the composites.

According to the results of chapter II, PDLLG75 showed favorable ion release and degradation behaviors comparing with other polymer matrices. These characteristics are crucial to stimulate cell activation for tissue regeneration. In chapter III, for purpose of controlling the ion release of SiV effectively to have an application in filling irregular shaped bone voids, soft and thin layer (~2 μm) of PDLLG75 was coated on the SiV/PLLA composite fibers by coaxial electrospinning. Obtaining cotton-wool-like materials with core-shell structure fibers was one of the significant objectives in this thesis, as this kind of material was expected to improve the mechanical flexibility and ion release of the SiV/PLLA composite fibers. The

mechanically flexible, recovery-ability and the ion-release behavior (in TBS) of the material was estimated.

Ions released from SiV could also play an important role in soft tissue regeneration. In chapter IV, for purpose of regulating the bone-like crystal (usually apatite) formation to prevent the calcification of soft tissue, and also controlling the ion release of SiV effectively, a coaxial electrospinning process was engineered to apply PDLLG coating on the fibres with SiV enclosed within a bio-inert polymeric matrix (PLLA). By careful selection of the electrospinning parameters, the diameter-thickness of shell layer could be modulated. The relationship between the rate of ion release and shell-thickness was discussed in detail. The apatite-formation abilities and the mechanical properties of the fibermats were investigated.

Reference

[1] S. J. Forbes, N. Rosenthal, Preparing the ground for tissue regeneration: from mechanism to therapy. *Nat. Med.*, **20**, 857-869 (2014).

[2] D. S. Thoma, B. Buranawat, C. H. F. Hämmerle, U. Held, R. E. Jung, Efficacy of soft tissue augmentation around dental implants and in partially edentulous areas: a systematic review. *J. Clin. Periodont.*, **41**, S77-S91 (2014).

[3] S. M. Zakaria, S. H. Sharif Zein, M. R. Othman, F. Yang, J. A. Jansen, Nanophase hydroxyapatite as a biomaterial in advanced hard tissue engineering: a review. *Tissue Eng. Part B: Reviews*, **19**, 431-441 (2013).

[4] M. W. Mariscalco, R. A. Magnussen, D. Mehta, T. E. Hewett, D. C. Flanigan, C. C. Kaeding, Autograft versus nonirradiated allograft tissue for anterior cruciate ligament reconstruction. *Am. J. Sport. Med.*, **42**, 492-499 (2014).

[5] R. Mascarenhas, B. J. Erickson, E. T. Sayegh, N. N. Verma, B. J. Cole, C. Bush-Joseph, B. R. Bach, Is there a higher failure rate of allografts compared with autografts in anterior cruciate ligament reconstruction: a systematic review of overlapping meta-analyses. *Arthroscopy: J. Arthroscop. Relat. Surg.*, **31**, 364-372 (2015).

[6] Y. Ge, H. Li, H. Tao, Y. Hua, J. Chen, S. Chen, Comparison of tendon–bone healing between autografts and allografts after anterior cruciate ligament reconstruction using magnetic resonance imaging. *Knee Surg., Sport. Traumat., Arthrosc.*, **23**, 954-960 (2015).

[7] T. W. Bauer, G. F. Muschler, Bone graft materials: an overview of the basic science. *Clin. Orthopaed. Relat. Res.*, **371**, 10-27 (2000).

[8] P. V. Giannoudis, H. Dinopoulos, E. Tsiridis, Bone substitutes: an update. *Injury*, **36**, S20-S27 (2005).

[9] A. Kolk, J. Handschel, W. Drescher, D. Rothamel, F. Kloss, M. Blessmann, M. Heiland, K. D. Wolff, R. Smeets, Current trends and future perspectives of bone substitute materials – from space holders to innovative biomaterials. *J. Cranio-Maxillof. Surg.*, **40**, 706-718 (2012).

[10] F. McCormick, J. D. Harris, G. D. Abrams, K. E. Hussey, H. Wilson, R. Frank, A. K. Gupta, J. Bernard R. Bach, B. J. Cole, Survival and reoperation rates after meniscal sllograft transplantation. *Am. J. Sport. Med.*, **42**, 892-897 (2014).

[11] S. L. Sherman, J. Garrity, K. Bauer, J. Cook, J. Stannard, W. Bugbee, Fresh osteochondral allograft transplantation for the knee: current concepts. *J. Am. Acade. Orthopaed. Surg.*, **22**, 121-133 (2014).

[12] V. T. Athanasiou, D. J. Papachristou, A. Panagopoulos, A. Saridis, C. D. Scopa, P. Megas, Histological comparison of autograft, allograft-DBM, xenograft, and synthetic grafts in a trabecular bone defect: an experimental study in rabbits. *Med. Sci. Moni.*, **16**, 24-31 (2009).

[13] K. R. Stone, U. Galili, Controversies in the technical aspects of ACL reconstruction, Springer, 343-353 **(**2017).

[14] K. Komiya, S. Nasuno, K. Uchiyama, N. Takahira, N. Kobayashi, H. Minehara, S. Watanabe, M. Itoman, Status of bone allografting in Japan – nation-wide survey of bone grafting performed from 1995 through 1999. *Cell Tissue Bank.*, **4**, 217-220 (2003).

[15] F. Edalat, I. Sheu, S. Manoucheri, A. Khademhosseini, Material strategies for creating artificial cell-instructive niches. *Curr. Opin. Biotechnol.*, **23**, 820-825 (2012).

[16] A. S. Greenwald, S. D. Boden, V. M. Goldberg, Y. Khan, C. T. Laurencin, R. N. Rosier, Bone-graft substitutes: facts, fictions, and applications. *J. Bone Joint Surg.*, **83**, 98-103 (2001).

[17] R. Sridharan, A. R. Cameron, D. J. Kelly, C. J. Kearney, F. J. O'Brien, Biomaterial based modulation of macrophage polarization: a review and suggested design principles. *Mater. Today*, **18**, 313-325 (2015).

[18] R. A. Perez, S.-J. Seo, J.-E. Won, E.-J. Lee, J.-H. Jang, J. C. Knowles, H.-W. Kim, Therapeutically relevant aspects in bone repair and regeneration. *Mater. Today*, **18**, 573-589 (2015).

[19] A. C. Jones, C. H. Arns, A. P. Sheppard, D. W. Hutmacher, B. K. Milthorpe, M. A. Knackstedt, Assessment of bone ingrowth into porous biomaterials using MICRO-CT. *Biomaterials*, **28**, 2491-2504 (2007).

[20] S. C. Cox, J. A. Thornby, G. J. Gibbons, M. A. Williams, K. K. Mallick, 3D printing of porous hydroxyapatite scaffolds intended for use in bone tissue engineering applications. *Mater. Sci. Eng.: C*, **47**, 237-247 (2015).

[21] S. Wu, X. Liu, K. W. K. Yeung, C. Liu, X. Yang, Biomimetic porous scaffolds for bone tissue engineering. *Mater. Sci. Eng.: R: Reports*, **80**, 1-36 (2014).

[22] Y. Liu, J. Lim, S.-H. Teoh, Review: Development of clinically relevant scaffolds for vascularised bone tissue engineering. *Biotechnol. Adv.*, **31**, 688-705 (2013).

[23] G. J. Owens, R. K. Singh, F. Foroutan, M. Alqaysi, C.-M. Han, C. Mahapatra, H.-W. Kim, J. C. Knowles, Sol–gel based materials for biomedical applications. *Prog. Mater. Sci.*, **77**, 1-79 (2016).

[24] A. Feinle, M. S. Elsaesser, N. Husing, Sol-gel synthesis of monolithic materials with hierarchical porosity. *Chem. Soc. Rev.*, **45**, 3377-3399 (2016).

[25] A. Greiner, J. H. Wendorff, Electrospinning: a fascinating method for the preparation of ultrathin fibers. *Angew. Chem. Int. Ed.*, **46**, 5670-5703 (2007).

[26] Y. He, G. Xue, J. Fu, Fabrication of low cost soft tissue prostheses with the desktop 3D printer. *Sci. Rep.*, **4**, 6973 (2014).

[27] P. X. Ma, R. Langer, Tissue Engineering Methods and Protocols (Eds.: J. R. Morgan, M. L. Yarmush), Humana Press, Totowa, NJ, 47-56 (1999).

[28] V. J. Chen, P. X. Ma, Nano-fibrous poly(l-lactic acid) scaffolds with interconnected spherical macropores. *Biomaterials*, **25**, 2065-2073 (2004).

[29] M. M. Martino, P. S. Briquez, K. Maruyama, J. A. Hubbell, Extracellular matrix-inspired growth factor delivery systems for bone regeneration. *Adv. Drug. Deliv. Rev.*, **94**, 41-52 (2015).

[30] A. Hayrapetyan, J. A. Jansen, J. J. J. P. van den Beucken, Signaling pathways involved in osteogenesis and their application for bone regenerative medicine. *Tissue Eng. Part B: Reviews*, **21**, 75-87 (2014).

[31] D. H. R. Kempen, L. B. Creemers, J. Alblas, L. Lu, A. J. Verbout, M. J. Yaszemski, W. J. A. Dhert, Growth factor interactions in bone regeneration. *Tissue Eng. Part B: Reviews*, **16**, 551-566 (2010).

[32] A. Malhotra, C. van Blitterswijk, P. Habibovic, Biology and Engineering of Stem Cell Niches (Ed.: J. M. Karp), Academic Press, Boston, 499-516 (2017).

[33] N. J. Lakhkar, I.-H. Lee, H.-W. Kim, V. Salih, I. B. Wall, J. C. Knowles, Bone formation controlled by biologically relevant inorganic ions: role and controlled delivery from phosphate-based glasses. *Adv. Drug. Deliv. Rev.*, **65**, 405-420 (2013).

[34] A. Hoppe, N. S. Güldal, A. R. Boccaccini, A review of the biological response to ionic dissolution products from bioactive glasses and glass-ceramics. *Biomaterials*, **32**, 2757-2774 (2011).

[35] S. Haimi, G. Gorianc, L. Moimas, B. Lindroos, H. Huhtala, S. Räty, H. Kuokkanen, G. K. Sándor, C. Schmid, S. Miettinen, R. Suuronen, Characterization of zinc-releasing three-dimensional bioactive glass scaffolds and their effect on human adipose stem cell proliferation and osteogenic differentiation. *Acta Biomater.*, **5**, 3122-3131 (2009).

[36] T. Kasuga, Bioactive calcium pyrophosphate glasses and glass-ceramics. *Acta Biomater.*, **1**, 55-64 (2005).

[37] A. M. Smith, R. E. Baker, D. Kay, P. K. Maini, Incorporating chemical signalling factors into cell-based models of growing epithelial tissues. *J. Mathemat. Biol.*, **65**, 441-463 (2012).

[38] C. Brose, D. Schmitt, H. von Briesen, M. Reimann, Directed differentiation of pancreatic stem cells by soluble and immobilised signalling factors. *Ann. Anatom. - Anatom. Anz.*, **191**, 83-93 (2009).

[39] M. Carvalho-Gaspar, J. S. Billing, B. M. Spriewald, K. J. Wood, Chemokine gene expression during allograft rejection: comparison of two quantitative PCR techniques. *J. Immunol. Methods*, **301**, 41-52 (2005).

[40] J. O. Hollinger, A. O. Onikepe, J. MacKrell, T. Einhorn, G. Bradica, S. Lynch, C. E. Hart, Accelerated fracture healing in the geriatric, osteoporotic rat with recombinant human platelet-derived growth factor-bb and an injectable beta-tricalcium phosphate/collagen matrix. *J. Orthop. Res.*, **26**, 83-90 (2008).

[41] X. Liu, P. X. Ma, Polymeric scaffold for bone tissue engineering. *Ann. Biomed. Eng.*, **32**, 477-486 (2004).

[42] P. X. Ma, Scaffolds for tissue fabrication. *Mater.s Today*, **7**, 30-40 (2004).

[43] J. F. Mano, R. A. Sousa, L. F. Boesel, N. M. Neves, R. L. Reis, Bioinert, biodegradable and injectable polymeric matrix composites for hard tissue replacement: state of the art and recent developments. *Comp. Sci. Technol.*, **64**, 789-817 (2004).

[44] A. Obata, S. Tokuda, T. Kasuga, Enhanced in vitro cell activity on silicon-doped vaterite/poly(lactic acid) composites. *Acta Biomater.*, **5**, 57-62 (2009).

[45] K. Rezwan, Q. Z. Chen, J. J. Blaker, A. R. Boccaccini, Biodegradable and bioactive porous polymer/inorganic composite scaffolds for bone tissue engineering. *Biomaterials*, **27**, 3413-3431 (2006).

[46] J. M. S Ramakrishna, Composites science and technology-biomedical applications of polymer-composite materials a review. *Comp. Sci. Technol.*, **61**, 1189-1224 (2001).

[47] B. Guo, P. X. Ma, Synthetic biodegradable functional polymers for tissue engineering: a brief review. *Sci. China Chem.*, **57**, 490-500 (2014).

[48] P. Gentile, V. Chiono, I. Carmagnola, P. V. Hatton, An overview of poly(lactic-*co*-glycolic) acid (PLGA)-based biomaterials for bone tissue engineering. *Int. J. Mol. Sci.*, **15**, 3640-3659 (2014).

[49] K. Rezwan, Q. Z. Chen, J. J. Blaker, A. R. Boccaccini, Biodegradable and bioactive porous polymer/inorganic composite scaffolds for bone tissue engineering. *Biomaterials*, **27**, 3413-3431 (2006).

[50] F. Torres, S. Nazhat, S. Sheikhmdfadzullah, V. Maquet, A. Boccaccini, Mechanical properties and bioactivity of porous PLGA/TiO_2 nanoparticle-filled composites for tissue engineering scaffolds. *Comp. Sci. Technol.*, **67**, 1139-1147 (2007).

[51] C. J. Bettinger, E. J. Weinberg, K. M. Kulig, J. P. Vacanti, Y. Wang, J. T. Borenstein, R. Langer, Three-dimensional microfluidic tissue-engineering scaffolds using a flexible biodegradable polymer. *Adv. Mater.*, **18**, 165-169 (2005).

[52] L. E. V.-N. Freed, Gordana; Biron, Robert J., Biodegradable polymer scaffolds for tissue engineering. *Bio/Technology*, **12**, 689-693 (1994).

[53] S. Giovagnoli, P. Blasi, M. Ricci, A. Schoubben, L. Perioli, C. Rossi, Physicochemical characterization and release mechanism of a novel prednisone biodegradable microsphere formulation. *J. Pharm. Sci.*, **97**, 303-317 (2008).

[54] L. Gui, L. Zhao, R. W. Spencer, A. Burghouwt, M. S. Taylor, S. W. Shalaby, L. E. Niklason, Development of novel biodegradable polymer scaffolds for vascular tissue engineering. *Tissue Eng. Part A*, **17**, 1191-1200 (2011).

[55] H. K. Makadia, S. J. Siegel, Poly lactic-*co*-glycolic acid (PLGA) as biodegradable controlled drug delivery carrier. *Polymers (Basel)*, **3**, 1377-1397 (2011).

[56] P. Nooeaid, W. Li, J. A. Roether, V. Mourino, O. M. Goudouri, D. W. Schubert, A. R. Boccaccini, Development of bioactive glass based scaffolds for controlled antibiotic release in bone tissue engineering via biodegradable polymer layered coating. *Biointerphases*, **9**, 041001 (2014).

[57] H. Maeda, T. Kasuga, L. L. Hench, Preparation of poly(l-lactic acid)-polysiloxane-calcium carbonate hybrid membranes for guided bone regeneration. *Biomaterials*, **27**, 1216-1222 (2006).

[58] A. Obata, T. Hotta, T. Wakita, Y. Ota, T. Kasuga, Electrospun microfiber meshes of silicon-doped vaterite/poly(lactic acid) hybrid for guided bone regeneration. *Acta Biomater.*, **6**, 1248-1257 (2010).

[59] H. Maeda, T. Kasuga, Control of silicon species released from poly(lactic acid)-polysiloxane hybrid membranes. *J. Biomed. Mater. Res. Part A*, **85A**, 742-746 (2008).

[60] H. Maeda, K. Kato, T. Kasuga, Adsorption behavior of proteins on calcium silicate hydrate in Tris and phosphate buffer solutions. *Mater. Lett.*, **167**, 112-114 (2016).

[61] S. Yamada, H. Maeda, A. Obata, U. Lohbauer, A. Yamamoto, T. Kasuga, Cytocompatibility of siloxane-containing vaterite/poly(l-lactic acid) composite coatings on metallic magnesium. *Materials*, **6**, 5857 (2013).

[62] J. Nakamura, G. Poologasundarampillai, J. R. Jones, T. Kasuga, Tracking the formation of vaterite particles containing aminopropyl-functionalized silsesquioxane and their structure for bone regenerative medicine. *J. Mater. Chem. B*, **1**, 4446-4454 (2013).

[63] S. Yamada, Y. Ota, J. Nakamura, Y. Sakka, T. Kasuga, Preparation of siloxane-containing vaterite doped with magnesium. *J. Ceram. Soc. Jpn*, **122**, 1010-1015 (2014).

[64] S. Yamada, A. Obata, H. Maeda, Y. Ota, T. Kasuga, Development of magnesium and siloxane-containing vaterite and its composite materials for bone regeneration. *Front. Bioeng. Biotechnol.*, **3**, 195 (2015).

[65] C. Xu, P. Su, X. Chen, Y. Meng, W. Yu, A. P. Xiang, Y. Wang, Biocompatibility and osteogenesis of biomimetic bioglass-collagen-phosphatidylserine composite scaffolds for bone tissue engineering. *Biomaterials*, **32**, 1051-1058 (2011).

[66] P. Han, C. Wu, Y. Xiao, The effect of silicate ions on proliferation, osteogenic differentiation and cell signalling pathways (WNT and SHH) of bone marrow stromal cells. *Biomater. Sci.*, **1**, 379-392 (2013).

[67] A. Manchón, M. Alkhraisat, C. Rueda-Rodriguez, J. Torres, J. C. Prados-Frutos, A. Ewald, U. Gbureck, J. Cabrejos-Azama, A. Rodriguez-González, E. López-Cabarcos, Silicon calcium phosphate ceramic as novel biomaterial to simulate the bone regenerative properties of autologous bone. *J. Biomed. Mater. Res. Part A*, **103**, 479-488 (2015).

[68] S. K. Yoo, C. M. Freisinger, D. C. LeBert, A. Huttenlocher, Early redox, Src family kinase, and calcium signaling integrate wound responses and tissue regeneration in zebrafish. *J. Cell Biol.*, **199**, 225–234 (2012).

[69] K. Kawai, B. J. Larson, H. Ishise, A. L. Carre, S. Nishimoto, M. Longaker, H. P. Lorenz, Calcium-based nanoparticles accelerate skin wound healing. *PLoS One*, **6**, e27106 (2011).

[70] M. Ducharme-Desjarlais, C. J. Cáeste, É. Lepault, C. L. Theoret, Effect of a silicone-containing dressing on exuberant granulation tissue formation and wound repair in horses. *Am. J. Vet. Res.*, **66**, 1133-1139 (2005).

[71] S. Yoshizawa, A. Brown, A. Barchowsky, C. Sfeir, Magnesium ion stimulation of bone marrow stromal cells enhances osteogenic activity, simulating the effect of magnesium alloy degradation. *Acta Biomater.*, **10**, 2834-2842 (2014).

Chapter II Dissolution behavior of Mg/Si-doped vaterite particles in biodegradable polymer composites

1 Introduction

Tissue engineering scaffolds play a decisive role in the repair and regeneration of bones [1–4]. These scaffolds provide a supporting matrix and an essential environment for cells to attach, spread, proliferate, differentiate, and mineralize. Scaffolds consisting of biodegradable polymers and bioactive materials have attracted great research attention because they can combine the tailored degradability of polymers with the osteoconductivity of bioactive materials [2, 3]. Bioactive materials, such as Bioglass® 45S5, combined with lactic acid-based polymers, showed impressive bone-forming ability [5, 6].

The ions released from 45S5 have been reported to stimulate the attachment, proliferation, differentiation, and mineralization of osteoblastic cells *in vitro* and angiogenesis both *in vitro* and *in vivo* [7–9]. The calcium (Ca^{2+}) and silicate ions released from 45S5 can stimulate osteoblast cell division and the production of growth factors and extracellular matrix proteins [9–11]. Ca^{2+} ions are necessary for bone remodeling since they directly activate intercellular mechanisms by affecting the calcium-sensing receptors in osteoblastic cells [12]. In aqueous solutions, silicate ions are associated with the formation and calcification of bone tissue [13, 14]. Magnesium (Mg^{2+}) ions have been reported to stimulate cellular activity, especially the adhesion of osteoblasts [15, 16]. These stimulatory effects on cellular activities play an important role in bone regeneration.

From these reports, it can be inferred that materials capable of releasing Mg^{2+}, Ca^{2+}, and silicate ions might be beneficial as new biomaterials. In our previous work, siloxane-containing calcium carbonate (vaterite) doped with magnesium (MgSiV) was developed [17, 18]. MgSiV particles had distorted spherical shapes with a diameter of ~1.3 μm and a thickness of ~0.6 μm; they were capable of releasing Ca^{2+}, Mg^{2+}, and silicate ions in aqueous solutions. The ions released from MgSiV are expected to promote cell adhesion, proliferation, and differentiation. The ion releasing behavior of MgSiV in aqueous solutions has been reported in our earlier work [17]; it was observed that the ions were released in a short period of time. The rapid release might cause pH instability and have a significant effect on homeostasis. We propose that MgSiV can be used as a filler in polymeric composites. The ion releasing behavior of MgSiV-containing composites has not been examined so far to the best of our knowledge.

In this work, lactic acid-based polymers, such as poly(L-lactic acid) (PLLA) and poly(D,L-lactide-*co*-glycolide) (PDLLG), were used as the matrix polymers to prepare the composites with MgSiV particles as the fillers. PLLA and PDLLG belong to the family of linear aliphatic polyesters, which are often used to prepare bioactive composites. The extra methyl group in the PLLA repeating unit reduces its molecular affinity to water and leads to a slow degradation [24]. PDLLG with its higher fraction of glycolide units is likely to hydrate and swell faster than PLLA and also to degrade faster [19–22]. This work focuses on the Mg^{2+}, Ca^{2+}, and silicate ion release from MgSiV-PLLA and MgSiV-PDLLG composites in Tris buffer solutions (TBS). Changes in the surface morphologies of the composites and pH values of the solutions are also discussed.

2 Experimental section

2.1 Raw materials

Poly(L-lactic acid) (PLLA) (LACEA, Mitsui Chemicals Co. Ltd., Japan) and two kinds of poly(D,L-lactide-*co*-glycolide) (PDLLG) (Purasorb®; lactide : glycolide = 75 : 25 and 50 : 50; Corbion Purac Biomaterials, The Netherlands) were used in this work. According to the ratio of lactide to glycolide in PDLLG (75 : 25 and 50 : 50), they were named as PDLLG75 and PDLLG50, respectively. The molecular weights of PLLA, PDLLG75, and PDLLG50 were 140, 170, and 170 kDa, respectively.

MgSiV particles were prepared using a carbonation method described in our previous report [17]. Briefly, 133.4 g of $Ca(OH)_2$ was dissolved in a co-solvent containing 2000 mL of methanol and 200 mL of distilled water (DW). After CO_2 gas was blown in the solution for 20 min, 11.7 g of $Mg(OH)_2$ and 60 mL of 3-aminopropyltriethoxysilane (APTES) were added into the slurry, which was stirred for another 40 min while CO_2 was being blown. The resulting slurry was dried at 110 ^oC to obtain MgSiV particles (diameter ~1 μm). The silicon and magnesium contents of the MgSiV particles were estimated to be 2.8 mass% and 2.0 mass% by inductively coupled plasma atomic emission spectroscopy (ICP-AES).

2.2 Preparation of MgSiV-polymer composite films

To prepare the MgSiV-polymer composites, MgSiV particles were initially kneaded with the polymers. The ratio of polymer to MgSiV was 53 : 47 (vol%) (40 : 60 in mass%). 28 g of the polymer was poured into a pre-heated kneading reactor and held for 5 min for melting and then 42 g of the MgSiV particles was added into the reactor

and kneading was carried out for 15 min. The processing temperatures were set at 190 ^{o}C for PLLA, 130 ^{o}C for PDLLG75, and 110 ^{o}C for PDLLG50.

A solution-casting method was employed to prepare the composite films. Four grams of the kneaded composites were dissolved in 40 g of chloroform and stirred in a capped vessel for 6 h at room temperature. The MgSiV-polymer composite solution was poured into a glass culture dish (ϕ = 90 mm) to evaporate the solvent. After the cast solutions were dried for 1 d, composite films with ~0.3 mm thickness were obtained. The resulting composite films are denoted as MgSiV-PLLA, MgSiV-PDLLG75, and MgSiV-PDLLG50.

2.3 Surface morphologies

The surface and fracture morphologies of the composite films were observed using a scanning electron microscope (SEM, JSM-6301F, JEOL, Japan) after the specimens were coated with a thin layer of platinum. The cross-sections, obtained by breaking the films soaked in liquid nitrogen for 2 min with tweezers, were observed to analyze the fracture face morphologies. To characterize the crystalline phases, X-ray diffraction (XRD, X'pert X-ray diffractometer, Philips; Cu$K\alpha$, 50 kV, 40 mA) was carried out. The scanning rate was 1 $^{o}\cdot$min^{-1}.

2.4 Ion release behavior

The ion releasing behavior of the composite films was evaluated in TBS as described previously [17]. The preparation of TBS was carried out as follows – initially, 6.118 g of tris(hydroxymethyl) aminomethane was dissolved in 1000 mL distilled water

at 37 ^{o}C and the pH of the solution was adjusted to 7.4 with 1 M hydrochloric acid. To examine the dissolution behavior of the composite films, each film of ~ 0.3 mm-thickness was cut into square-shaped samples (20 mm × 20 mm), which were soaked in 10 mL TBS in a polystyrene vessel. The vessel was sealed and stored statically in an incubator at 37 ^{o}C. At predetermined time intervals (1 h ~ 7 d), the soaked samples were taken out from the solution, rinsed with DW, and dried at room temperature; meanwhile, the Mg^{2+}, Ca^{2+}, and silicate ion contents in the solutions were analyzed. The experiments were performed in triplicate at each time point for statistical relevance.

The concentrations of the Mg^{2+}, Ca^{2+}, and silicate ions in the solutions after soaking the samples were measured by ICP-AES (ICPS-500, Shimadzu, Japan). Calibration curves were generated using magnesium, calcium, and silicon standard solutions at 1, 10, and 50 mg·mL^{-1}. The pH values of the solutions were measured using a potentiometric pH meter (F-73T, HORIBA Ltd., Japan) at room temperature.

3 Results and discussion

3.1 Surface morphology

Figure 2–1 shows the SEM images of the composites before and after being soaked in TBS. Before the samples were soaked, MgSiV particles were found to be spread on the film surfaces homogeneously.

Immediately after soaking the films in TBS, MgSiV particles on the film surface started to dissolve. After 1 h, the amount of particles decreased and numerous pores, which were comparable in size with the particles (~1 μm), were observed on the

surfaces. These phenomena are thought to originate from the rapid dissolution of MgSiV particles on the surface of the composite films, which were covered with a thin polymer layer that would dissolve within 1 h; during soaking, the thin polymer layers were rapidly hydrolyzed and degraded and the particles could dissolve in the solution.

After 1 d, new needle-like products precipitated on the surface of the samples. In the case of MgSiV-PLLA, there were almost no changes in the sizes and number of surface pores while the number of needle-like products increased. In the case of PDLLG-based composites, after day 3, the number of ~1 μm-sized pores decreased and larger pores appeared, which implies the degradation of PDLLG matrices. After day 3, numerous cube-like products were observed on MgSiV-PDLLG50.

Figure 2–2 shows the XRD patterns of the composites before and after soaking them in TBS. The patterns clearly show the phase transformation of calcium carbonate crystals. Before soaking, the composites were characterized by the strong diffraction peaks originating from vaterite phase in the MgSiV particles, containing a small amount of calcite [23]. After 1 d of soaking, the peak intensities of vaterite in all the samples reduced and peaks corresponding to aragonite appeared. The new needle-like products are believed to be aragonite crystals. After 7 d of soaking, strong peaks corresponding to aragonite were observed in the diffractograms of MgSiV-PLLA and MgSiV-PDLLG75. It has been reported that aragonite is formed in a carbonation process when the aqueous solution contains Mg^{2+} ions [24–27]. The existence of Mg^{2+} ions in the solution modifies the nucleation kinetics in the crystallization process of calcium carbonates. The growth rate of calcite decreases while that of aragonite is unaffected [26, 27]. In the case of MgSiV-PDLLG50, after 7 d of soaking, strong diffraction peaks corresponding to calcite were observed. The cube-like products are

believed to be calcite crystals. The XRD patterns and the surface morphologies (Figure 2–1) suggest that, at day 7, calcite was the dominant crystal phase in MgSiV-PDLLG50.

3.2 Ion release behavior

Figure 2–3 shows the cumulative amounts of Mg^{2+}, Ca^{2+}, and silicate ions released from the composite films after they were soaked in TBS. Silicate ion release was measured in terms of silicon ion release from a calibration curve generated using the standard solution for ICP-AES.

The amount of Mg^{2+} ions released from the PDLLG-based composite films increased rapidly within 3 d, after which the release was almost constant due to discontinuous release. In other words, almost all of the Mg^{2+} ions embedded in the PDLLG-based samples were dissolved within 3 d of soaking in TBS. On the other hand, in the case of Mg^{2+} ion release from MgSiV-PLLA, the cumulative release amounts were always smaller than those of the PDLLG-based samples; furthermore, a continuous increase in the amount of the released Mg^{2+} ions was observed. After 7 d of soaking, ~70 % of the magnesium in the intact sample was estimated to have been released. The Mg^{2+} ion release behavior might originate from the chemical structure of MgSiV. During processing, Mg^{2+} ions form Mg–O–Si bonds and aggregate on the surface of calcium carbonate through a deprotonated OH group bonding with Ca^{2+} ions [17, 28]. Ca^{2+} ions were released rapidly from MgSiV-PLLA and MgSiV-PDLLG75 within 12 h (~10 % of calcium content in the original samples); after day 1, the released Ca^{2+} ion content decreased and was almost constant until 7 d. In the case of MgSiV-PDLLG50, Ca^{2+} ions were released rapidly within 12 h, and the released contents were high at day 3 and day 7. The silicate ion release behavior was similar to

that of Mg^{2+} ion. Within 3 d, almost all of the silicate ions were released (80 ~ 100 % of silicon content in the original samples). In the case of MgSiV-PLLA, the release of silicate ions was suppressed relatively after 12 h.

The rapid release of the silicate ions within 12 h is considered to be due to the dissolution of the MgSiV particles on the surfaces of the films. Immediately after the films were exposed to TBS, dissolution started. For example, consider the case of MgSiV-PDLLG75. As shown in Figure 2–4, at hour 1, a homogeneous distribution of the MgSiV particles could be seen on the surface; pores were formed when these particles dissolved. The composites include ~50 vol% MgSiV particles, which are embedded in the polymer matrix phase and some of the particles might be in contact with other particles. When the particles dissolved, pores were left in the matrix and continuous pores, if any, transformed into channels. In our previous work [29], when PDLLG75 was coated on a material with Ca^{2+} and silicate ion release capability, the resulting material's release kinetics followed the Weibull model, showing a purely diffusive release after the hydration of the PDLLG75 layer. In this work, because of the water uptake ability of PDLLGs, the MgSiV particles embedded tightly in the polymer matrix dissolve and ions diffuse through both the channel and the PDLLG matrix. After day 3, almost no MgSiV particles could be observed and some new products formed inside the porous sample. In the case of PDLLG-based composites, it is believed that the absorption-diffusion model comes into play immediately after the films are soaked in TBS.

In Figure 2–3, slight decreases in the cumulative amounts of Mg^{2+} and silicate ions were observed. Although this might be in the region of measurement error, the

possibility of adsorption to form new products around the sample surface might be also considered. Experiment for clarifying this phenomenon is in progress.

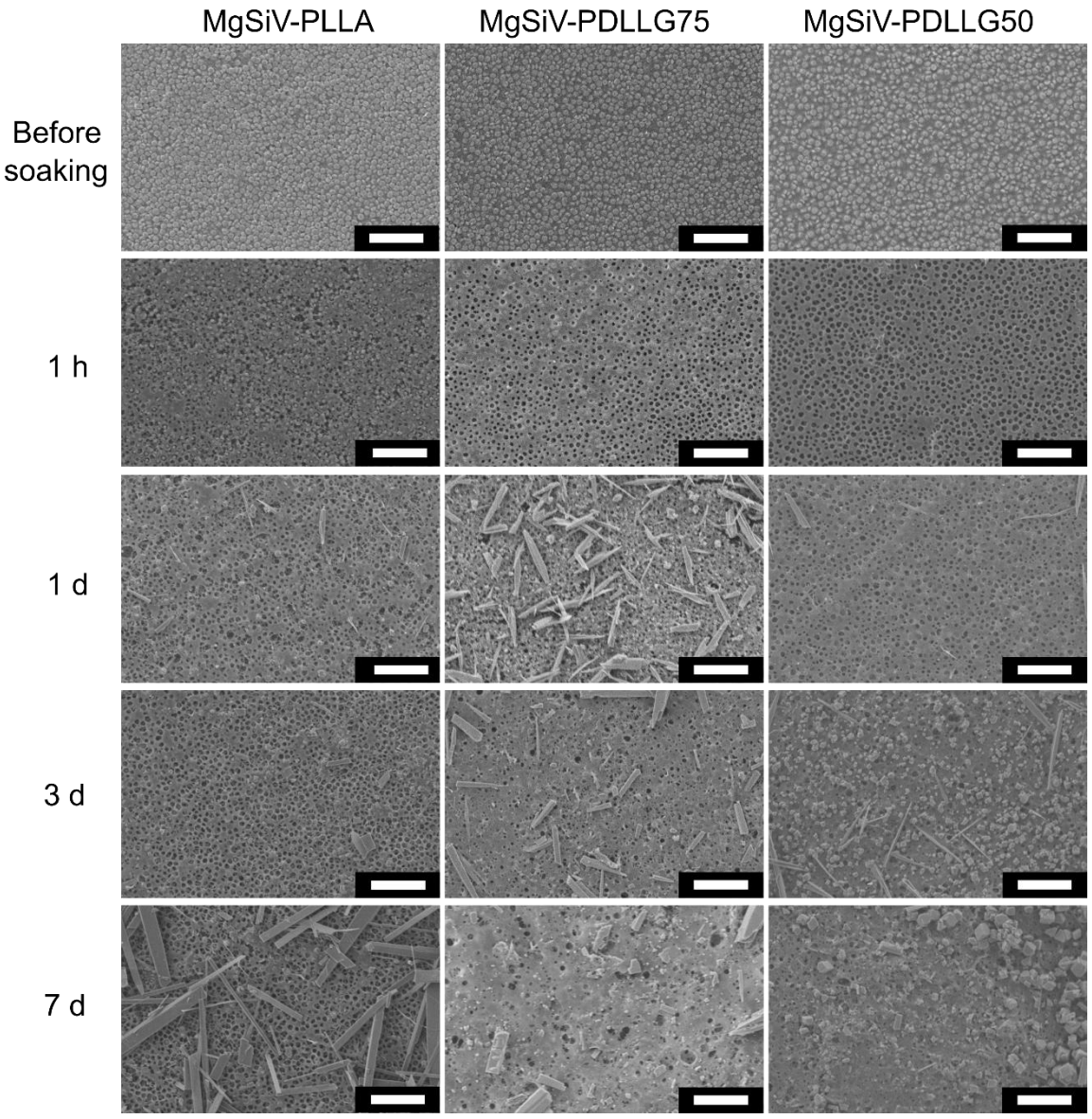

Fig. 2–1. SEM images of the composite films before and after soaking in TBS for 1 h ~ 7 d. The scale bar is 10 μm.

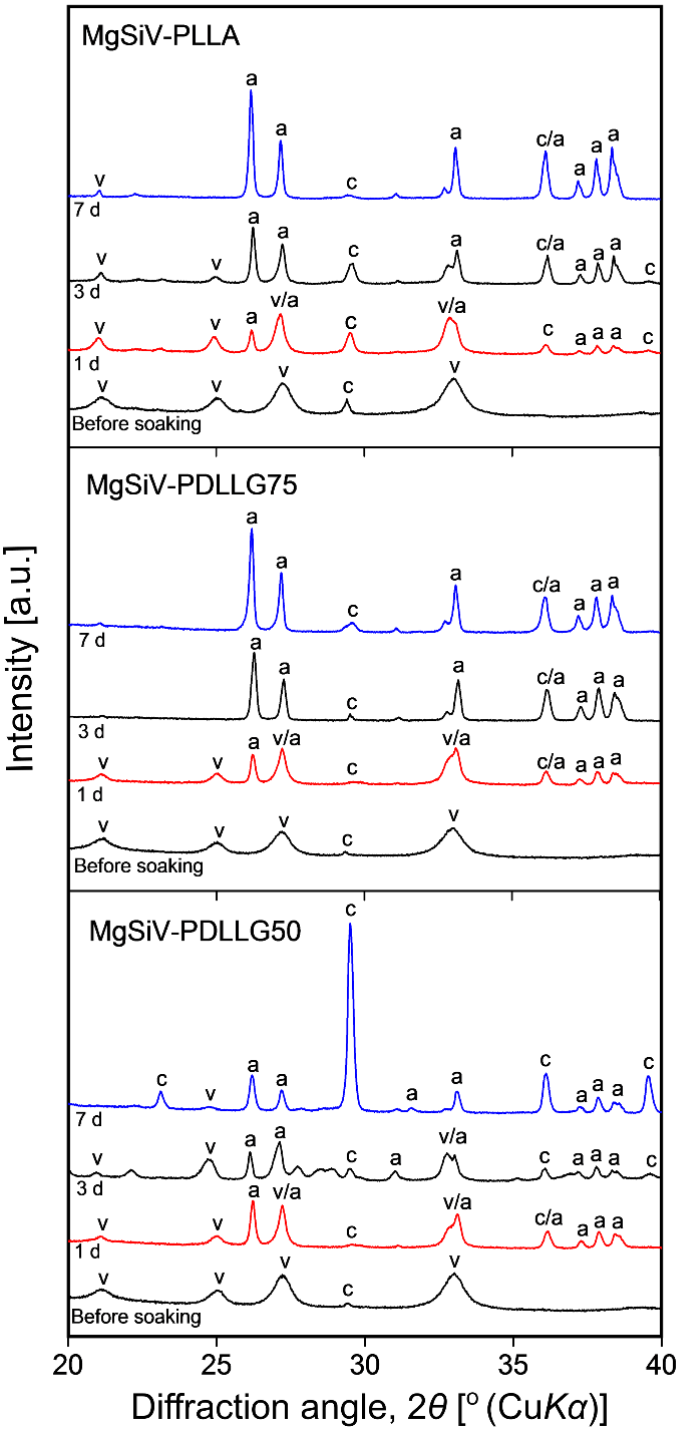

Fig. 2–2. XRD patterns of the composite films before and after soaking in TBS for 7 d. a = aragonite, v = vaterite, and c = calcite.

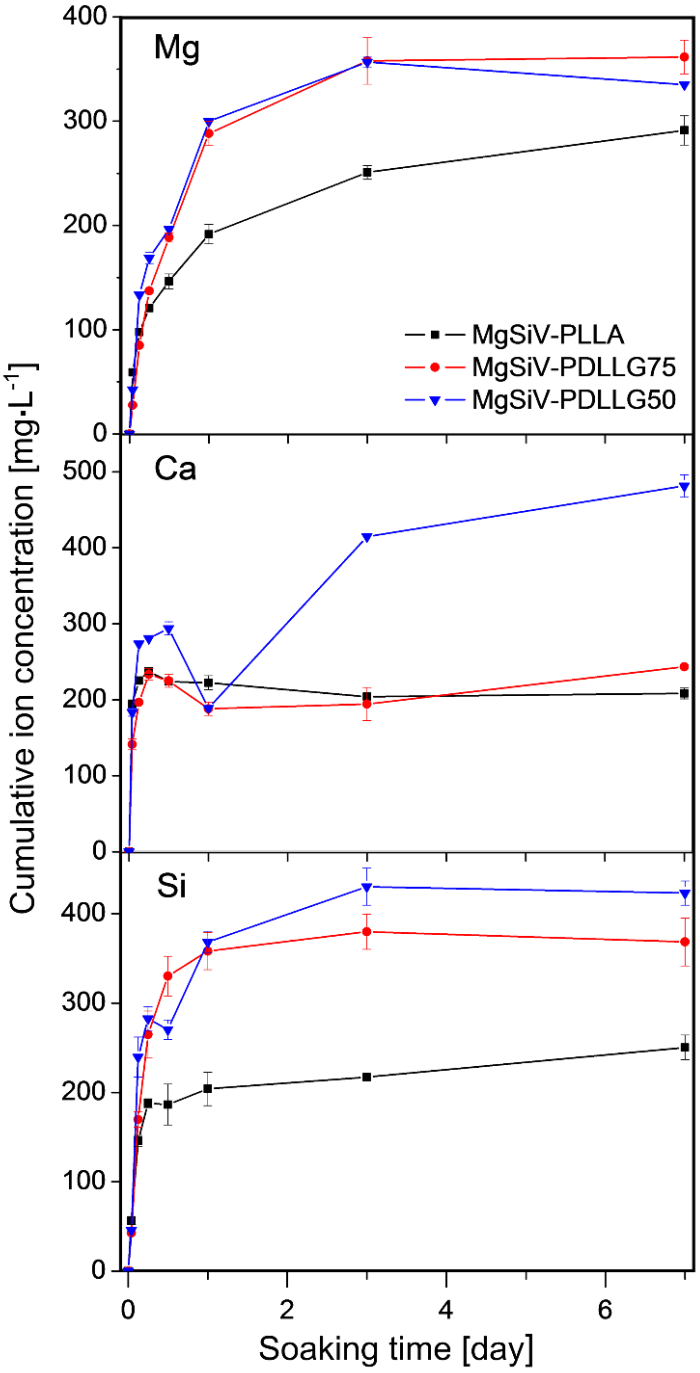

Fig. 2–3. Mg^{2+}, Ca^{2+}, and silicate ions release profiles after soaking the composite films in TBS at 37 ℃. The error bars indicate standard deviation.

The amount of ions released from MgSiV-PLLA was smaller than that from PDLLG-based samples. This would be due to the strong hydrophobicity and low degradability of PLLA. The extra methyl group in the PLLA repeating unit reduces its molecular affinity to water and leads to slow hydrolysis [30]. Therefore, the penetration of TBS into the composite is very slow and it takes a long time for the particles embedded in the PLLA matrix to be exposed to TBS. As a result, the release of ions is controlled. The routes for ion release from MgSiV-PLLA are believed to be developed by the dissolution of MgSiV particles on the surface and agglomerated ones; thus, the absorption-diffusion model cannot suitably explain the release behavior in this case.

Figure 2–5 shows the pH values of TBS after soaking the samples. In the case of MgSiV-PLLA and MgSiV-PDLLG75, the values increased until day 3. Mg^{2+}, Ca^{2+}, and silicate ions released from the MgSiV particles on the surface would increase the pH value of TBS. As a result, the degradation of PLLA and PDLLG75 might be promoted slightly [20]. As the released ion content reduced after 3 ~ 7 d, the pH values were almost constant. In Figure 2–3, the cumulative amounts of Ca^{2+} ions released from the composites were found to increase up to 12 h of soaking, after which they decreased to ~200 $mg \cdot L^{-1}$, which then remained constant. After 1 d, the formation of aragonite took place (Figures 2–1 and 2–2). Aragonite has been reported to form in Mg^{2+} ion-containing aqueous solutions at pH > ~8 with needle-like shapes [24]. In other words, Ca^{2+} ions released from MgSiV were consumed to form aragonite crystals.

On the other hand, the solution in which MgSiV-PDLLG50 was soaked, exhibited different Ca^{2+} ion content and pH values (in Figures 2–3 and 2–5, respectively). PDLLG50 has been reported to have the highest degradability among the various PDLLG systems available [22]. The decrease in the pH of the solution is

considered to be due to the rapid hydrolysis of the polymer chains [20]. As a result, the release of Ca^{2+} ions is accompanied by a decrease in the pH. After 7 d of soaking, the pH of the solution was around 7.5 (<8). During the precipitation of calcium carbonate polymorphs, solutions with high Mg/Ca ratios tend to precipitate aragonite while those with low ratios tend to form calcite [27]. In the case of MgSiV-PDLLG50, after 1 d, the low pH would enhance the release of Ca^{2+}. As a result, the Mg/Ca ratio in the solution decreased, thus favoring calcite formation.

As described earlier, the rate of ion release from MgSiV-PLLA was slower as compared to PDLLG-based composites due to the poor water uptake ability and slow degradation rate of the PLLA matrix. Therefore, to rapidly release Mg^{2+} ions and enhance cell adhesion, PDLLG-based composites would be preferable.

However, when MgSiV-PDLLG50 is used in the body, the fast degradation of PDLLG50 would lead to a dramatic decrease in the pH of the environment around the material. The high water uptake and swelling ability of PDLLG50 could lead to wide channels and pathways, which can enhance the interaction of the particles with aqueous solutions and facilitate ion diffusion. It should also be kept in mind that the large variations in pH and amount of ions released might limit the application of these materials in bone repair.

In contrast, MgSiV-PDLLG75 is expected to exhibit a suitable ion release behavior. A large portion of the Mg^{2+} ions were dissolved out within 3 d. Ca^{2+} ions were released continuously and consumed in aragonite formation. This behavior is expected to have a beneficial effect on cell adhesion. After 3 d, the silicate ion release was almost controlled. Obata *et al.* reported that when an appropriate amount of silicate ions was supplied only at the initial stages of cell culture, mineralization could be enhanced [31].

Such phenomena are caused by the formation of pathways for ion release, originating from the water uptake ability of the polymer. As shown in Figure 2–1, MgSiV-PDLLG75 exhibited a healing effect on the small-sized pores on its surface after 1 d. Since the pH values after soaking MgSiV-PDLLG75 in TBS increased moderately to 7.8–8.1, no negative effect on bone-forming ability would be given.

For effectively stimulating cell activation for bone repair, the material used should exhibit desirable ion release and degradation characteristics. In this context, MgSiV-PDLLG75 is expected to be a promising candidate for bone repair. Advanced applications to medical devices with drug delivery systems using MgSiV-PDLLG75 would be also expected. The devices might be derived via various techniques, such as protein-entrapping [32], electrospinning [33], sol-gel processing [34], hydrogelation [35] and oil-spill treatment [36].

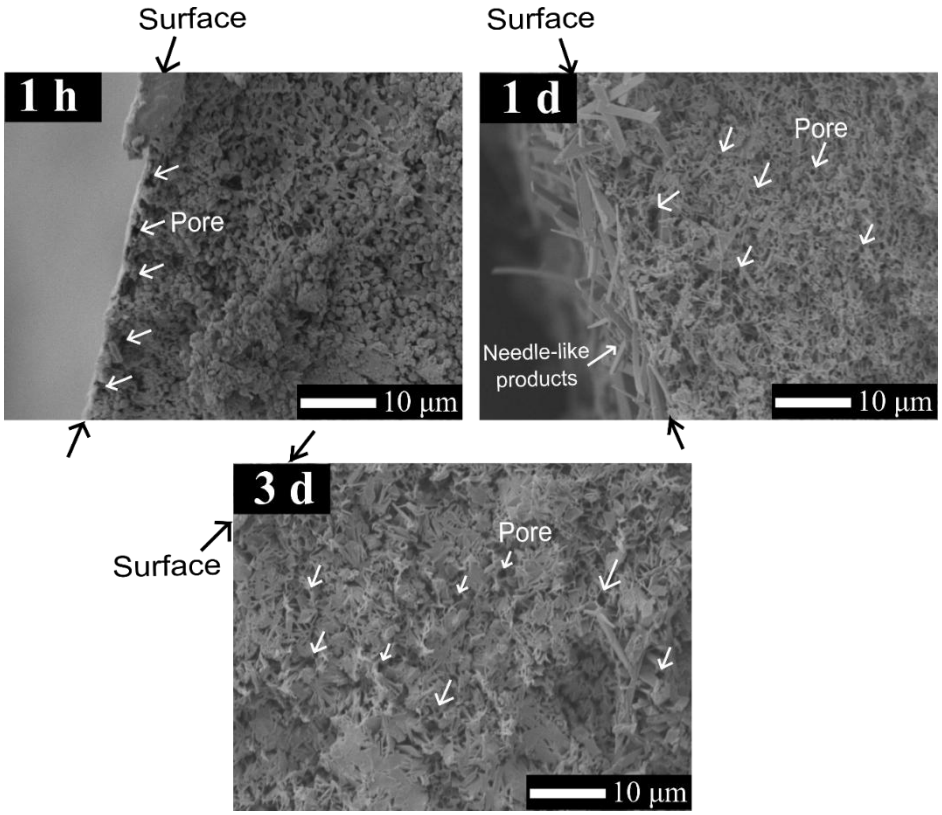

Fig. 2–4. Cross-sectional SEM images of MgSiV-PDLLG75 fracture samples after films were soaked in TBS for 1 h, 1 d, and 3 d.

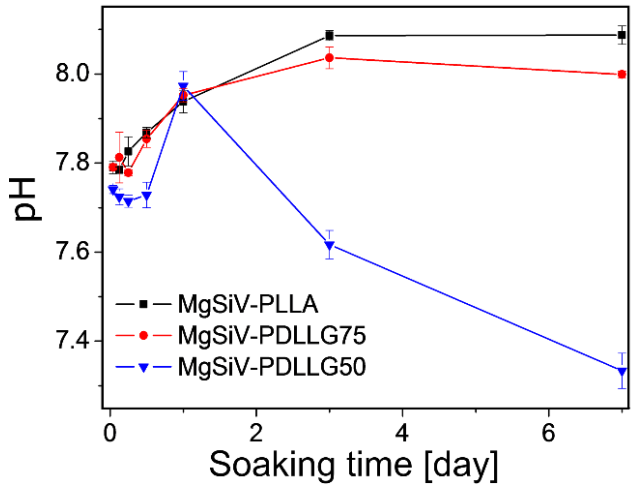

Fig. 2–5. The pH values of TBS (at 37 ^{o}C) after soaking the composite films. The error bars indicate standard deviation.

4 Conclusions

- Three kinds of composites containing MgSiV particles were prepared using PLLA, PDLLG75, and PDLLG50 as the polymeric matrices.
- The release of Mg^{2+}, Ca^{2+}, and silicate ions from these composites in TBS was investigated. The strong hydrophobicity of PLLA controlled the release of ions from the MgSiV-PLLA composite. The fast degradation of PDLLG50 induced a decrease in the pH of the TBS soaking solution.
- During a 7 d period, MgSiV-PDLLG75 composites exhibited continuous ion release and the pH of the soaking solution was found to be steady; these composites exhibited desirable water uptake ability and degradability, which helps in the creation of pathways for ion release and diffusion. Therefore, it is concluded that MgSiV in combination with PDLLG75 is suitable for use in bone repair applications.

References

[1] P. X. Ma, Scaffolds for tissue fabrication. *Mater. Today*, **7**, 30-40 (2004).

[2] A. R. Amini, C. T. Laurencin, S. P. Nukavarapu, Bone tissue engineering: recent advances and challenges. *Cri. Rev. Biomed. Eng.*, **40**, 363-408 (2012).

[3] S. Bose, S. Tarafder, Calcium phosphate ceramic systems in growth factor and drug delivery for bone tissue engineering: a review. *Acta Biomater.*, **8**, 1401-1421 (2012).

[4] P. Gentile, V. Chiono, I. Carmagnola, P. V. Hatton, An overview of poly (lactic-co-glycolic) acid (PLGA)-based biomaterials for bone tissue engineering. *Int. J. Mol. Sci.*, **15**, 3640-3659 (2014).

[5] G. Vergnol, N. Ginsac, P. Rivory, S. Meille, J. M. Chenal, S. Balvay, J. Chevalier, D. J. Hartmann, *In vitro* and *in vivo* evaluation of a polylactic acid-bioactive glass composite for bone fixation devices. *J. Biomed. Mater. Res. Part B: Appl. Biomater.*, **104B**, 180-191 (2016).

[6] S. Verrier, J. J. Blaker, V. Maquet, L. L. Hench, A. R. Boccaccini, PDLLA/Bioglass® composites for soft-tissue and hard-tissue engineering: an in vitro cell biology assessment. *Biomaterials*, **25**, 3013-3021 (2004).

[7] O. Tsigkou, L. L. Hench, A. R. Boccaccini, J. M. Polak, M. M. Stevens, Enhanced differentiation and mineralization of human fetal osteoblasts on PDLLA containing Bioglass® composite films in the absence of osteogenic supplements. *J. Biomed. Mater. Res. Part A*, **80A**, 837-851 (2007).

[8] O. Tsigkou, J. R. Jones, J. M. Polak, M. M. Stevens, Differentiation of fetal osteoblasts and formation of mineralized bone nodules by 45S5 Bioglass® conditioned medium in the absence of osteogenic supplements. *Biomaterials*, **30**, 3542-3550 (2009).

[9] I. D. Xynos, A. J. Edgar, L. D. Buttery, L. L. Hench, J. M. Polak, Gene-expression profiling of human osteoblasts following treatment with the ionic products of Bioglass® 45S5 dissolution. *J. Biomed. Mater. Res.*, **55**, 151-157 (2001).

[10] J. R. Jones, Review of bioactive glass: From Hench to hybrids. *Acta Biomater.*, **9**, 4457-4486 (2013).

[11] A. Hoppe, N. S. Güldal, A. R. Boccaccini, A review of the biological response to ionic dissolution products from bioactive glasses and glass-ceramics. *Biomaterials*, **32**, 2757-2774 (2011).

[12] P. J. Marie, The calcium-sensing receptor in bone cells: a potential therapeutic target in osteoporosis. *Bone*, **46**, 571-576 (2010).

[13] C. Maniatopoulos, J. Sodek, A. H. Melcher, Bone formation in vitro by stromal cells obtained from bone marrow of young adult rats. *Cell Tissue Res.*, **254**, 317-330 (1988).

[14] M. Mastrogiacomo, A. Papadimitropoulos, A. Cedola, F. Peyrin, P. Giannoni, S. G. Pearce, M. Alini, C. Giannini, A. Guagliardi, R. Cancedda, Engineering of bone using bone marrow stromal cells and a silicon-stabilized tricalcium phosphate bioceramic: evidence for a coupling between bone formation and scaffold resorption. *Biomaterials*, **28**, 1376-1384 (2007).

[15] H. Zreiqat, C. R. Howlett, A. Zannettino, P. Evans, G. Schulze-Tanzil, C. Knabe, M. Shakibaei, Mechanisms of magnesium-stimulated adhesion of osteoblastic cells to commonly used orthopaedic implants. *J. Biomed. Mater. Res.*, **62**, 175-184 (2002).

[16] S. Yoshizawa, A. Brown, A. Barchowsky, C. Sfeir, Magnesium ion stimulation of bone marrow stromal cells enhances osteogenic activity, simulating the effect of magnesium alloy degradation. *Acta Biomater.*, **10**, 2834-2842 (2014).

[17] S. Yamada, Y. Ota, J. Nakamura, Y. Sakka, T. Kasuga, Preparation of siloxane-containing vaterite doped with magnesium. *J. Ceram. Soc. Jpn.*, **122**, 1010-1015 (2014).

[18] S. Yamada, A. Obata, H. Maeda, T. Kasuga, Development of magnesium and siloxane-containing vaterite and its composite materials for bone regeneration. *Front. Bioeng. Biotechnol.*, **3**, 195/1-195/9 (2015).

[19] X. S. Wu, Synthesis, characterization, biodegradation, and drug delivery application of biodegradable lactic/glycolic acid polymers: Part III. Drug delivery application. *Artif. Cells Blood Substit. Biotechnol.*, **32**, 575-591 (2004).

[20] F. Alexis, Factors affecting the degradation and drug−release mechanism of poly (lactic acid) and poly [(lactic acid)−*co*−(glycolic acid)]. *Polym. Int.*, **54**, 36-46 (2005).

[21] J. M. Anderson, M. S. Shive, Biodegradation and biocompatibility of PLA and PLGA microspheres. *Adv. Drug Deliv. Rev.*, **64**, 72-82 (2012).

[22] I. Carmagnola, T. Nardo, P. Gentile, C. Tonda-Turo, C. Mattu, S. Cabodi, P. Defilippi, V. Chiono, Poly(lactic acid)-based blends with tailored

physicochemical properties for tissue engineering applications: a case study. *Int. J. Polym. Mater.*, **64**, 90-98 (2015).

[23] C. G. Kontoyannis, N. V. Vagenas, Calcium carbonate phase analysis using XRD and FT-Raman spectroscopy. *Analyst,* **125**, 251-255 (2000).

[24] Y. Ota, S. Inui, T. Iwashita, T. Kasuga, Y. Abe, Preparation of aragonite whiskers. *J. Am. Ceram. Soc.*, **78**, 1983-1984 (1995).

[25] L. Fernandez-Diaz, A. Putnis, The role of magnesium in the crystallization of calcite and aragonite in a porous medium. *J. Sediment. Res.*, **66**, 482-491 (1996).

[26] E. Loste, R. M. Wilson, R. Seshadri, F. C. Meldrum, The role of magnesium in stabilising amorphous calcium carbonate and controlling calcite morphologies. *J. Cryst. Growth*, **254**, 206-218 (2003).

[27] V. De Choudens-Sanchez, L. A. Gonzalez, Calcite and aragonite precipitation under controlled instantaneous supersaturation: elucidating the role of $CaCO_3$ saturation state and Mg/Ca ratio on calcium carbonate polymorphism. *J. Sediment. Res.*, **79**, 363-376 (2009).

[28] J. Nakamura, G. Poologasundarampillai, J. R. Jones, T. Kasuga, Tracking the formation of vaterite particles containing aminopropyl-functionalized silsesquioxane and their structure for bone regenerative medicine. *J. Mater. Chem. B,* **1**, 4446-4454 (2013).

[29] P. Zhou, J. Wang, A. L. Ma ϙon, A. Obata, J. R. Jones, T. Kasuga, Tailoring the delivery of therapeutic ions from bioactive scaffolds while inhibiting their apatite nucleation: a coaxial electrospinning strategy for soft tissue regeneration. *RSC Adv.*, **7**, 3992-3999 (2017).

[30] B. Damadzadeh, H. Jabari, M. Skrifvars, K. Airola, N. Moritz, P. K. Vallittu, Effect of ceramic filler content on the mechanical and thermal behaviour of poly-L-lactic acid and poly-L-lactic-co-glycolic acid composites for medical applications. *J. Mater. Sci. Mater. Med.*, **21**, 2523-2531 (2010).

[31] A. Obata, N. Iwanaga, A. Terada, G. Jell, T. Kasuga, Osteoblast-like cell responses to silicate ions released from 45S5-type bioactive glass and siloxane-doped vaterite. *J. Mater. Sci*., **52**, 8942-8956 (2017).

[32] V. L. Kudryavtseva, L. Zhao, S. I. Tverdokhlebov, G. B. Sukhorukov, Fabrication of PLA/$CaCO_3$ hybrid micro-particles as carriers for water-soluble bioactive molecules. *Colloids Surf. B Biointerfaces*, **157**, 481-489 (2017).

[33] L. Mei, Y. Wang, A. Tong, G. Guo, Facile electrospinning of an efficient drug delivery system. *Expert Opin. Drug Deliv.*, **13**, 741-753 (2016).

[34] R. Fan, X. Deng, L. Zhou, X. Gao, M. Fan, Y. Wang, G. Guo, Injectable thermosensitive hydrogel composite with surface-functionalized calcium phosphate as raw materials. *Int. J. Nanomedicine*, **9**, 615-626 (2014).

[35] H. Y. Yang, L. N. Niu, J. L. Sun, X. Q. Huang, D. D. Pei, C. Huang, F. R. Tay, Biodegradable mesoporous delivery system for biomineralization precursors. *Int. J. Nanomedicine*, **12**, 839-854 (2017).

[36] S. Kalliola, E. Repo, V. Srivastava, J. P. Heiskanen, J. A. Sirviö, H. Liimatainen, M. Sillanpää, The pH-sensitive properties of carboxymethyl chitosan nanoparticles cross-linked with calcium ions. *Colloids Surf. B Biointerfaces*, **153**, 229-236 (2017).

Chapter III Preparation of mechanically-flexible, cotton wool-like, bioresorbable composites with calcium and silicate ions-releasability

1 Introduction

Numerous works on bone regeneration using bioactive materials have been reported. In particular, recently much attention has been paid to bone tissue engineering. [1] Bone-void fillers are effective for the regeneration: various materials, such as hydroxyapatite, β-tricalcium phosphate, bioactive glass, and so on, have been commercialized as the fillers, which have connective porous structure. [2, 3]

Hench, *et al.* reviewed that calcium and silicate ions released from bioactive glasses implanted in bone-void show stimulatory effect on bone regeneration. [4, 5] These ions activate osteogenesis and angiogenesis through mediation by insulin-like growth factor (IGF), transforming growth factor β (TGF-β), bone morphogenic proteins (BMPs), vascular endothelial growth factor (VEGF) and so on. [6] Xynos, *et al*. reported that calcium and silicate ions increase the proliferation of human osteoblasts through gene activation. [7, 8]

Inorganic-organic composite scaffolds with controllable degradation and bioactive properties are receiving considerable interest for bone tissue regeneration. [9–11] In our group, some polymer–ceramic hybrids or composites with the ability to release calcium and silicate ions has been prepared for the regeneration. [12–14] One of the most promising materials among them is believed to be a composite consisting of poly($_L$-lactic acid) (PLLA) and siloxane-doped calcium carbonate (vaterite) (SiV)

particles, which are derived from aminopropyltriethoxysilane (APTES) and amorphous calcium carbonates (ACCs). [15] A siloxane group around the particle surfaces makes an amide-I bond to a carboxy group at the end of a PLLA chain and the Ca^{2+} ion in ACC is coordinated with carboxy groups: SiV particles in the composite are embedded tightly in the PLLA matrix [13]. The SiV-PLLA composite (denoted by SiVPC, hereafter) showed the release of calcium and silicate ions, and enhanced cells' proliferation and differentiation in culture tests using murine osteoblast-like MC3T3-E1 cells. [12, 13]

SiVPC can be easily shaped to long fibers with diameters of submicrometer to several tens micrometers using electrospinning. A kneaded mixture of PLLA and SiV particles at around 200 ^{o}C is dissolved in chloroform, and a high voltage source was utilized to inject charge of a certain polarity into the solution, which is accelerated toward a collector of the opposite polarity. As a result, nonwoven SiVPC can be obtained. [13]

The resulting SiVPC fibrous material containing 20 vol% (30 wt%) of SiV showed hydroxyapatite-forming ability by soaking in simulated body fluid (SBF), while that containing 47 vol% (60 wt%) of SiV exhibited the rapid the forming ability. [14] Numerous large spaces between the fibers in the nonwoven allowed cells' ingrowth and proliferation. *In vivo* test using New Zealand rabbits showed excellent bone formation around the fibers containing 47 vol% of SiV. [13]

For repairing irregular bone defects, bone filling materials with the shapes of granules or porous blocks are used during the healing process. If the materials are mechanically flexible, they would be receiving considerable interest. Although nonwoven materials are very promising for bone regeneration, their thickness would be

usually limited to 0.1~0.2 mm. In our earlier work, cotton wool-like SiVPCs have been developed by a modified electrospinning method. [16] From the view point of significance on *in vitro* bioactivity and animal tests above-mentioned, cotton wool-like SiVPC containing 47 vol% of SiV is expected to be one of the optimum materials. The fibers, however, are brittle due to the high SiV content and the cotton wool-like structure easily collapsed during handling.

One of the ideas for improving the mechanical brittleness is to choose the well-characterized biodegradable poly(D,L-lactide-*co*-glycolide) (PDLLG), which is a copolymer of poly(lactic acid) (PLA) and poly(glycolic acid) (PGA), as the matrix polymer in SiVPC. PDLLG is amorphous since the PLA and PGA polymer chains are not tightly packed. [17] Tensile properties, especially the ductility, could be expected to be improved by altering the matrix polymer from PLLA to PDLLG. Although the composite containing PDLLG as a matrix polymer exhibited better mechanical properties than SiVPC with PLLA matrix, almost all of silicate ion dissolved out at a burst initially after being soaked in aqueous solution. [14] This may be originate from the high hydrophilicity and degradability of PDLLG.

In the present work, we hypothesized that coating a SiVPC fiber containing 47 vol% of SiV with a thin PDLLG layer, that is, preparing a so-called “core-shell”-type structure, may resolve the above-described issues: since the thin PDLLG layer could prevent direct contact of SiVPC with water immediately after soaking the fiber in aqueous solution, the burst-release of silicate ion might be inhibited, and meanwhile the mechanical properties might be improved.

In the present work, a coaxial electrospinning technique was used for preparing the homogenous PDLLG coating layer. [18] The preparation method, the mechanical

properties and ions-releasing behaviors of the cotton wool-like materials were discussed.

2 Experimental Section

As degradable polymers for fibrous materials, PLLA (LACEA, Mitsui Chemicals, Co., Ltd. Japan; M_w = 140 kDa) and poly($_{D,L}$-lactide-*co*-glycolide) (PDLLG, lactide : glycolide = 75 : 25) (Purasorb®; Corbion Purac Biomaterials, The Netherlands, M_w = 195 kDa) were chosen. The SiV particles, which were supplied from Yabashi Industries, Japan, were prepared by a carbonation process with methanol, following our previous reports. [12, 13] The particles had spherical shapes of ~1.4 μm in diameter and the Si content in them was estimated to be 2.6 wt% by X-ray fluorescence analysis.

PLLA and SiV particles were kneaded mechanically at 200 ^oC for 10 min to prepare SiVPC. The ratio of PLLA : SiV was 53 : 47 in vol% (*i.e.*, 40 : 60 in wt%). The resulting composites were dissolved in chloroform (Wako Pure Chemical Industries, Japan) to prepare 8 wt% solution of PLLA in SiVPC. PDLLG was also dissolved in chloroform to prepare 15 wt% solution.

Figure 3–1 shows a schematic drawing of a coaxial electrospinning method in the present work: a concentrical metallic nozzle was used for the spinning. A jet was generated on the tip of droplet, and a core-shell-type fiber was formed after adjusting some conditions such as an applied electric field strength, the viscosity and flow rate of each solution, and so on. [23-25] In the present work, 10 kV of the voltage was applied for electrospinning to the concentrical nozzle at room temperature. Each solution was loaded into each syringe pump (FP-W-100, Melquest, Japan), where the inner diameters

of the core-side (*i.e.*, SiVPC) nozzle and the shell-side (*i.e.*, PDLLG) one were 0.5 and 1.10 mm, respectively. The flow rates of the core-side and shell-side solutions were 37.6 and 3.3 μL·min^{-1}, respectively.

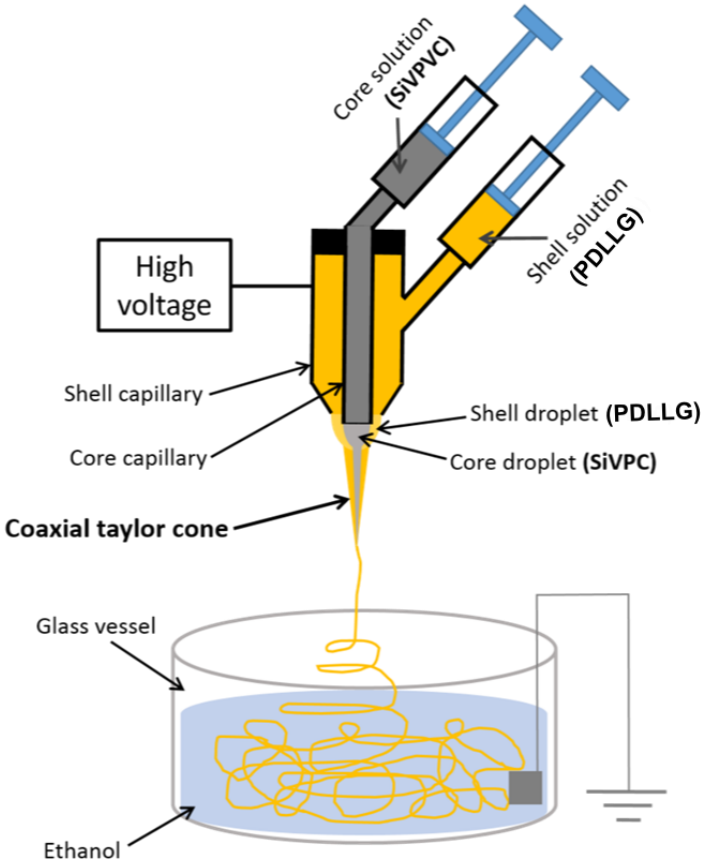

Fig. 3–1. Schematic drawing of a coaxial electrospinning for preparing cotton-wool-like materials.

A ground plate was soaked in ethanol and then placed in the vessel (100 mm in diameter). The distance between the concentrical nozzle and the vessel used as the collector was 150 mm. A high-tension field was applied to the nozzle. The impressed solution with core-shell-type structure flowed to the ground plate in the methanol, and chloroform was dissolved out to ethanol. As a result, the solution was solidified.

The resulting core-shell-type fibers in ethanol were collected and then washed with fresh ethanol, subsequently dried at room temperature, resulting in the formation of cotton wool-like materials.

Meanwhile, cotton wool-like SiVPC without the PDLLG-coating were prepared by electrospinning 12 wt% PLLA-solution containing SiV in chloroform at 15 kV of applied voltage into the above-described ethanol bath collector using a 18-gauge needle, as a control group.

The resulting fibers were observed by scanning electron microscopy (SEM; JSM-6301F, JEOL, Japan).

To evaluate the mechanical flexibility of the materials, their compression-recovery abilities were examined, following a modified JIS L1097 method. Fifty milligrams of each sample were filled in a glass bottle with an inner diameter of 15 mm and a height of 20 mm, and then a cover glass was placed on the sample. The height of the sample, h_1, was measured and subsequently a weight of 5.4, 16.2, or 27.0 g was placed on the sample and remained for 30 seconds, that is, the applied load was 0.3, 0.9, or 1.5 kPa, respectively. The height of the sample, h_2, was measured. The weight was removed and then the height of the sample, h_3, was measured 30 seconds after the removing. Compressibility (%), Z_1, and recovery ratio (%), Z_2, were estimated from the following equations, respectively:

$$Z_1 = \{(h_1 - h_2)/h_1 \times 100 \quad (1)$$

$$Z_2 = \{(h_3 - h_2)/(h_1 - h_2)\} \times 100 \quad (2)$$

The ions-releasabilities of the core-shell-type fibrous materials were examined using TBS (pH=7.4 at 36.5 ^{o}C). Twenty milligrams of the sample were soaked in the 10 mL of the solution at 36.5 ^{o}C for 32 days. At each time point, the sample was taken out from the solution. The amounts of calcium and silicate ions dissolved in the solution were measured by inductively coupled plasma-atomic emission spectroscopy (ICP-AES; ICPS-7000, Shimadzu, Japan) (n = 3).

3 Results and Discussion

3.1 Preparation of core-shell-type fibers

The preparation method of cotton wool-like materials has been reported in our earlier work. [16] In the present work, a coaxial electrospinning method was applied to this technique. Figure 3–2 shows an entire view and a scanning electron microscopic image (SEM image) of the resulting material. A large-sized cotton wool-like material of 20~30 mm thickness, not a fibermat, was obtained [Figure 3–2(a)]. It is easy to prepare the various-sized materials, dependently on the amount of jetted fibers. Many fibers, which were frizzled and independent of each other, provided high porosity with large-sized pores [Figure 3–2(b)].

Figure 3–3 shows the magnified SEM images of a fiber. The fiber diameters were ~10 μm. Many small-sized pits originating from the volatilization of solvent (chloroform) were observed on the surface [Figure 3–3(a)]. [19] In our earlier work, the diameter of electrospun fibers were reported to be one of the important parameters for

the cells' ingrowth. [20] The report showed that mouse osteoblast-like MC3T3-E1 cells on a PLLA fibermat could migrate and grow on fibers of ~10 μm in diameter three-dimensionally through gaps between them. On the other hand, in the case of the fibermat consisting of fibers with ~5 μm diameters, the cells grew two-dimensionally since the gap between fibers was too small for them to migrate. Therefore, the fiber diameters of the present cotton wool-like material were controlled to be ~10 μm, although they were changeable by choosing some spinning conditions such as the kind of solvent, viscosity, injecting speed, applied voltage, and so on.

The cross-sectional view of the fiber fractured in liquid nitrogen showed a core-shell-type structure [Figure 3–3(b)]. The core part, in which SiV particles in a PLLA matrix were observed, of ~8 μm diameter and the PDLLG coating layer of ~2 μm thickness were observed. It can be imaged from the fracture face that the SiVPC core fractured catastrophically and the PDLLG surface layer fractured after necking. A thin PDLLG layer has been successfully coated on the surface of SiVPC fibers without gaps between them. During the spinning process, PDLLG solution and SiVPC slurry are ejected out through different, coaxial capillary channels, forming a core-shell Taylor cone, and then it is forced by electrostatic potential, resulting in the formation of the "core-shell"-structured fiber. The advantage of this method is that the core fiber is uniformly coated with a thin layer.

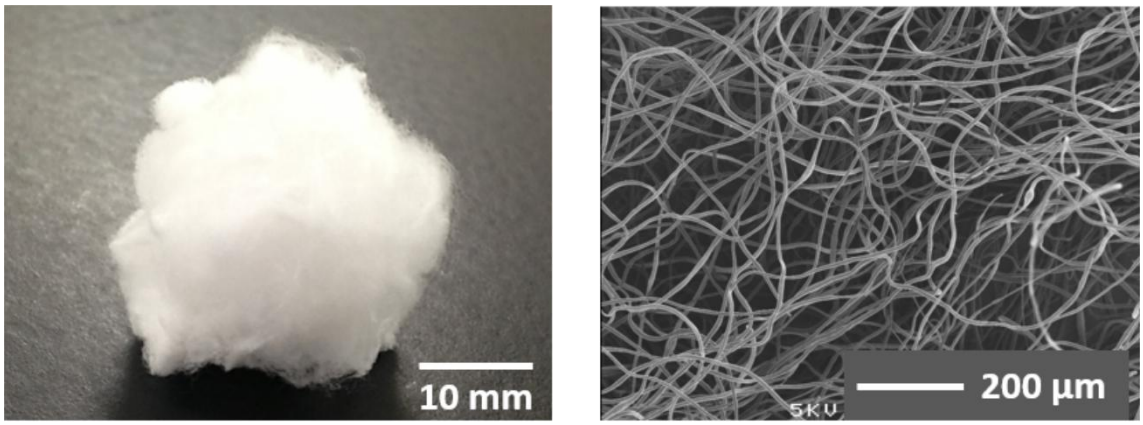

Fig. 3–2. (**a**) Entire view of the cotton wool-like material prepared using a coaxial electrospinning method; (**b**) SEM image of the material.

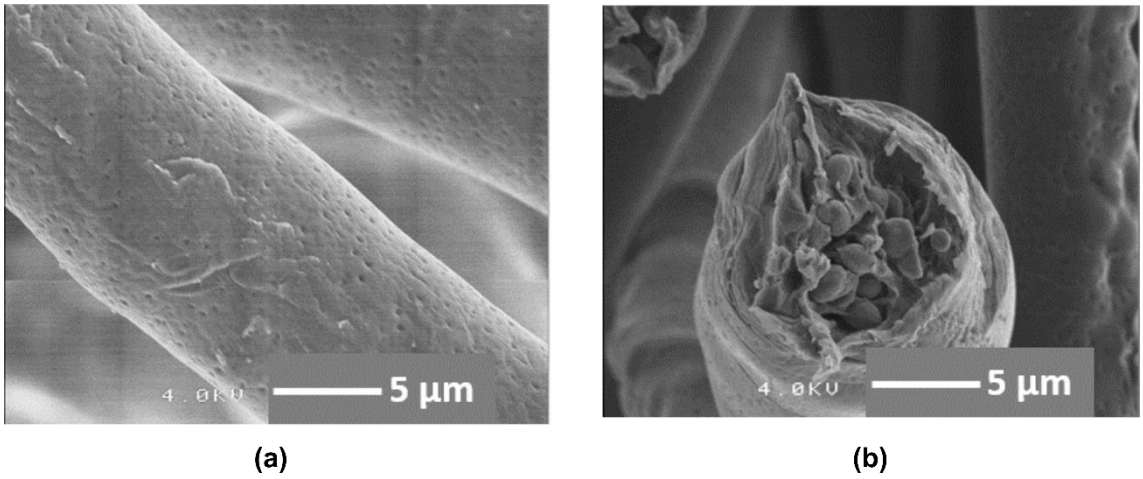

Fig. 3–3. SEM images of the resulting fibrous material using a coaxial electrospinning method. (**a**) The surface of the fiber; (**b**) Fracture face after breaking the fiber in liquid nitrogen.

3.2 Mechanical flexibility of cotton wool-like materials

Figure 3–4 shows the compressibilities and recovery ratios of the cotton wool-like materials, *i.e.*, SiVPC and PDLGA-coated SiVPC consisting of the "core-shell"-type fibers. The each compressibility increased with increasing the applied load, and they reached to ~60 % under 1.5 kPa of pressure. In the recovery test, although the samples showed ~60 % of the recovery ratio after removing 0.3 kPa of low pressure, SiVPC lost its recovering ability after pressing under 0.9 or 1.5 kPa due to its brittle fracture. On the other hand, PDLLG-coated SiVPC maintained ~50 % of the recovery ratio, even after pressing under 0.9 or 1.5 kDa.

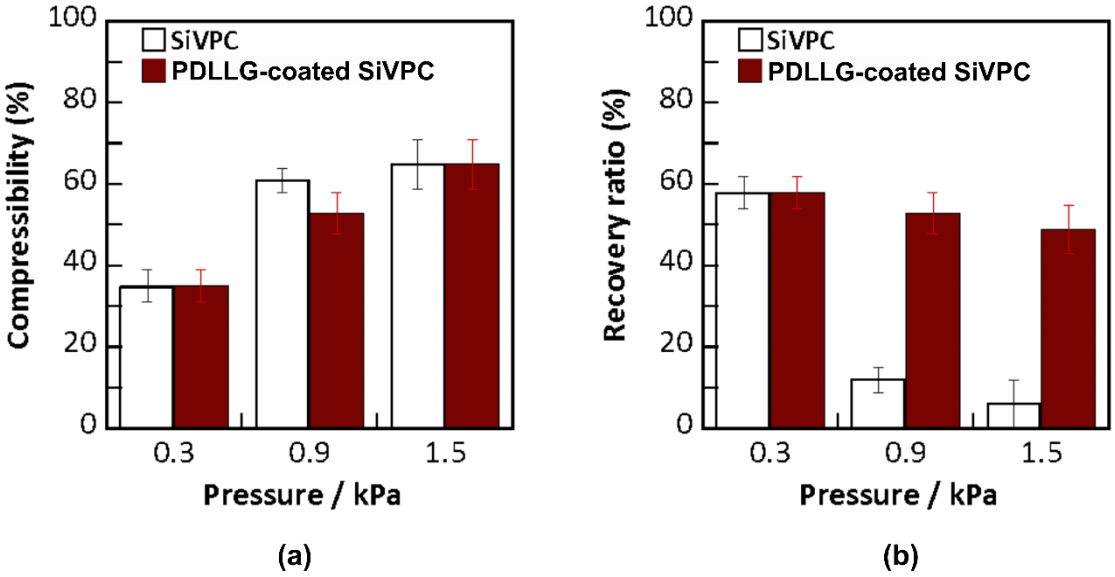

Fig. 3–4. (**a**) Compressibilities of cotton wool-like SiVPC and PDLLG-coated SiVPC; (**b**) Recovery ratios of the materials. An error bar shows a standard deviation ($n = 4$).

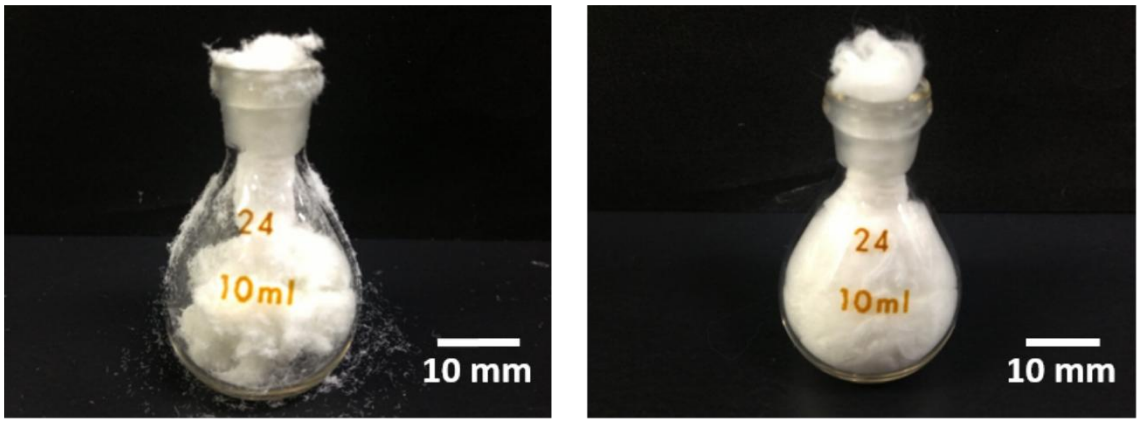

(a) (b)

Fig. 3–5. Entire views after cramming 500 g of cotton wool-like materials into a glass bottle (specific gravity bottle) of 10 mL. (a) SiVPC; (b) PDLLG-coated SiVPC.

Figure 3–5 shows the demonstration of handling performance using cotton wool-like SiVPC and PDLLG-coated SiVPC. Five hundred milligram of them were crammed into a glass bottle (specific gravity bottle) with 10 mL. The fibers of cotton wool-like SiVPC were broken during the cramming: the numerous small-sized broken fibers spilled, to be seen on a table and in the bottle: when the sample passed a narrow bottle mouth, it was compressed and many fibers were broken. Since the cotton wool-like SiVPC possessed poor recovering ability, there remained some space which was not filled with the fibers. On the other hand, cotton wool-like PDLLG-coated SiVPC showed the excellent mechanical flexibility, that is, it was deformed along the shape of the narrow mouth and the bottle was successfully filled completely.

It may be said that cotton wool-like PDLLG-coated SiVPC has excellent handling performance: this unique performance might play an important role as bone-void fillers.

3.3 Dissolution of calcium and silicate ions

Cotton wool-like SiVPC collapsed into very small-sized pieces after being soaked in TBS for 3 days at 36.5 ^{o}C, while the PDLLG-coated SiVPC maintained its shape even after being soaked for 32 days.

Figure 3–6 shows the cumulative percentages of the ions amounts dissolved in TBS from cotton wool-like SiVPC and PDLLG-coated SiVPC to total amounts of the ions in the materials before the soaking. The burst release of the ions from SiVPC was observed within 1 day: ~70 % of Ca^{2+} ion and ~98 % of silicate ion in the material were dissolved into the solution. On the other hand, in the case of the PDLLG-coated SiVPC, the initial release of the calcium and silicate ions after 1 day were controlled to ~23 and ~53 % (*i.e.*, ~45 and ~7 ppm), respectively. After that, the ions were released continuously in the present experimental span (*i.e.*, to 32 days). The PDLLG-coating is found to be effective for controlling the burst release of the ions and achieving their long-term release.

Calcium and silicate ions are known to be important elements for metabolic process associated with the formation and calcification of bone regeneration. [1–9] The control of the ions released from the materials is an important factor for enhancing their biological capability. In the present work, for the cotton wool-like SiVPC fibrous material without coating, almost all of silicate ion and ~70 % of calcium ion dissolved out within 1 day, that is, most of SiV particles dissolved, leaving a large amount of interconnected pores. As a result, the brittle porous fibers composed of a thin PLLA skeleton would be formed.

On the other hand, by being coated with a PDLLG layer around SiVPC, the release amount of the ions has been controlled successfully. From the morphology of

the resulting fibers, as shown in Figure 3–3 (a), all of the fibers were coated homogenously with a PDLLG layer, which included small-sized pits due to the volatilization of solvent (chloroform) during electrospinning. PDLLG is more hydrophilic than PLLA and likely to absorb water to swell. [21, 22] The good hydrophilicity and high degradation ability might allow the solution to permiate into the fibers, especially through around the pits. As a result, the ions could dissolve out in the solution. Then, by the swelling of PDLLG in the solution, the route would be narrowed and/or closed to control the ions release, resulting in the achivement of their long-term slow release.

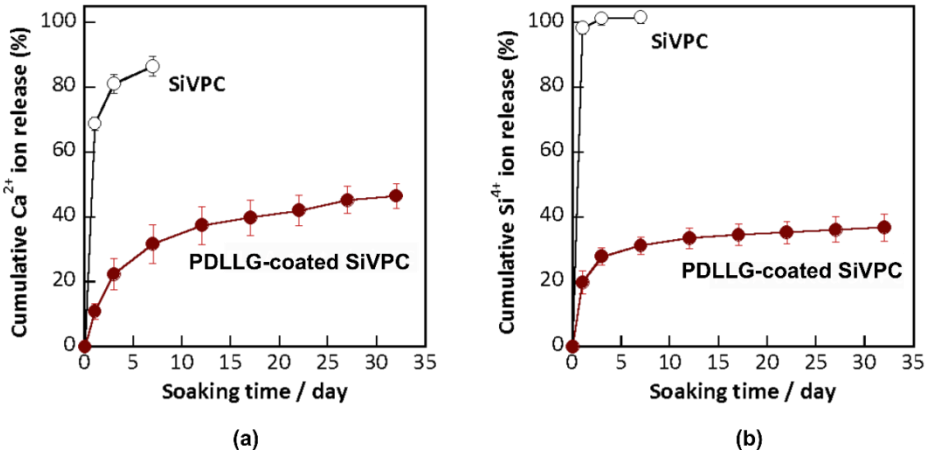

Fig. 3–6. Cumulative ion amounts dissolved from cotton wool-like materials as a function of soaking time. (**a**) Ca^{2+} ion; (**b**) Silicate ion (here, measured as Si^{4+} ion). An error bar shows a standard deviation ($n = 3$).

The core-shell-type fiber structure in the present work is concluded to be the excellent control system of ions release. The thickness of the coating layer should be one of the important factors for adjusting the ions-releasing behavior of the materials. Investigation on the control of the layer thickness is now in progress.

4 Conclusions

- Using a coaxial electrospinning technique, a PDLLG thin layer of ~2 μm-thickness has been successfully coated on the surface of SiVPC fibers of ~8 μm-diameter, which organized cotton wool-like structure.
- The SiVPC fibers without the coating were brittle to be easily broken into the small-sized fiber pieces under compressing, while the PDLLG-coated SiVPC fibers were mechanically tough to maintain their shape even after loading of 1.5 kPa. The mechanical flexibility of the cotton wool-like SiVPC was improved drastically by the thin PDLLG coating.
- This coating effectively controlled the initial burst release of calcium and silicate ions from SiVPC fibers in TBS. The SiVPC fibers collapsed in the solution within the 3 days, while the PDLLG-coated SiVPC ones maintained the structure even after being soaked in the solution for 1 month. Since the cotton wool-like “SiVPC-core/PDLLG-shell“-type material has highly-porous structure beneficial for cells migration, mechanical properties convenient for filling in irregular bone defects, and ions-releasing ability effective for enhancing cellular activities, it is expected to have an excellent performance in use as bone-void fillers.

References

[1] L. L. Hench, J. M. Polak, Third generation biomedical materials. *Science.* **295**, 1014-1017 (2002).

[2] W. S. Pietrzak, R. Ronk, Calcium sulfate bone void filler: a review and a look ahead. *J. Craniofacial Surg.*, **11**, 327-333 (2000).

[3] S. M. Kenny, M. Buggy, Bone cements and fillers: a review. *J. Mater. Sci. Mater. Med.*, **14**, 923-938 (2003).

[4] L. L. Hench, I. D. Xynos, J. M. Polak, Bioactive glasses for in situ tissue regeneration, *J. Biomater. Sci. Polym. Ed.*, **15**, 543-562 (2004).

[5] L. L. Hench, D. E. Day, W. Höland, V. M. Rheinberger, Glass and medicine, *Inter. J. Appl. Glass Sci.*, **1**, 104-117 (2010).

[6] A. Hoppe, N. S. Güldal, A. R. Boccaccini, A review of the biological response to ionic dissolution products from bioactive glasses and glass-ceramics. *Biomaterials*, **32**, 2757-2774 (2011).

[7] I. D. Xynos, A. J. Edgar, L. D. K. Buttery, L. L. Hench, J. M. Polak, Ionic products of bioactive glass dissolution increase proliferation of human osteoblasts and induce insulin-like growth factor II mRNA expression and protein synthesis. *Biochem. Biophys. Res. Commun.*, **276**, 461-465 (2000).

[8] I. D. Xynos, A. J. Edgar, L. D. K. Buttery, L. L. Hench, J. M. Polak, Gene-expression profiling of human osteoblasts following treatment with the ionic products of Bioglass® 45S5 dissolution. *J. Biomed. Mater. Res.*, **55**, 151-157 (2001).

[9] J. R. Jones, Review of bioactive glass: from hench to hybrids. *Acta Biomater.*, **9**, 4457-4486 (2013).

[10] W. Lu, K. Ji, J. Kirkham, Y. Yan, A. R. Boccaccini, M. Kellett, Y. Jin, X. Yang, *Cell Tissue Res.*, **356**, 97-107 (2014).

[11] A. R. Boccaccini, M. Erol, W. J. Stark, D. Mohn, Z. Hong, J. F. Mano, Polymer/bioactive glass nanocomposites for biomedical applications: a review. *Compos. Sci. Technol.*, **70**, 1764-1776 (2010).

[12] A. Obata, S. Tokuda, T. Kasuga, Enhanced in vitro cell activity on silicon-doped vaterite/poly(lactic acid) composites. *Acta Biomater.*, **5**, 57-62 (2009).

[13] A. Obata, T. Hotta, T. Wakita, Y. Ota, T. Kasuga, Electrospun microfiber meshes of silicon-doped vaterite/poly(lactic acid) hybrid for guided bone regeneration. *Acta Biomater.*, **6**, 1248-1257 (2010).

[14] K. Fujikura, A. Obata, S. Lin, J. R. Jones, R. V. Law, T. Kasuga, Preparation of electrospun poly(lactic acid)-based hybrids containing siloxane-doped vaterite particles for bone regeneration. *J. Biomater. Sci. Ploym. Ed.*, **23**, 1369-1380 (2012).

[15] J. Nakamura, G. Poologasundarampillai, J. R. Jones, T. Kasuga, Tracking the formation of vaterite particles containing aminopropyl-functionalized silsesquioxane and their structure for bone regenerative medicine, *J. Mater. Chem. B.*, **1**, 4446-4454 (2013).

[16] T. Kasuga, A. Obata, H. Maeda, Y. Ota, X. F. Yao, K. Oribe, Siloxane-poly(lactic acid)-vaterite composites with 3D cotton-like structure. *J. Mater. Sci: Mater. Med.*, **23**, 2349-2357 (2012).

[17] J. C. Middleton, A. J. Tipton, Synthetic biodegradable polymers as orthopedic devices. *Biomaterials.*, **21**, 2335-2346 (2000).

[18] Y. Su, X. Q. Li, H. S. Wang, C. L. He, X. M. Mo, Fabrication and characterization of biodegradable nanofibrous mats by mix and coaxial electrospinning. *J. Mater. Sci: Mater. Med.*, **20**, 2285-2294 (2009).

[19] Z. M. Huang, Y. Z. Zhang, M. Kotakic, S. Ramakrishna, A review on polymer nanofibers by electrospinning and their applications in nanocomposites. *Compos. Sci. Technol.*, **63**, 2223-2253 (2003).

[20] K. Fujikura, A. Obata, T. Kasuga, Cellular migration to electrospun poly(lactic acid) fibermats. *J. Biomater. Sci. Polym. Ed.*, **23**, 1939-1950 (2012).

[21] H. K. Makadia, S. J. Siegel, Poly lactic-*co*-glycolic acid (PLGA) as biodegradable controlled drug delivery carrier. *Polymers*, **3**, 1377-1397 (2011).

[22] X. Zong, S. Ran, K. S. Kim, D. Fang, B. S. Hsiao, B. Chu, Structure and morphology changes during in vitro degradation of electrospun poly(glycolide-*co*-lactide) nanofiber membrane. *Biomacromolecules*, **4**, 416-423 (2003).

[23] I. G. Loscertales, A. Barrero, M. Marquez, R. Spretz, R. Velarde-Ortiz, G. Larsen, Electrically forced coaxial nanojets for one-step hollow nanofiber design. *J. Am. Chem. Soc.*, **126**, 5376-5377 (2004).

[24] D. Li, Y. N. Xia, Direct fabrication of composite and ceramic hollow nanofibers by electrospinning. *Nano Lett.*, **5**, 933-938 (2004).

[25] J. E. Díaz, A. Barrero, M. Márquez, I. G. Loscertales, Controlled encapsulation of hydrophobic liquids in hydrophilic polymer nanofibers by co-electrospinning. *Adv. Funct. Mater.*, **16**, 2110-2116 (2006).

Chapter IV Tailoring the delivery of therapeutic ions from bioactive scaffolds while inhibiting their apatite nucleation: a coaxial electrospinning strategy for soft tissue regeneration

1 Introduction

Recently new biomaterials have been developed that can deliver therapeutic ions for the regeneration of soft tissues. [1–3] Enriching the local environment of human cells in ions such as calcium or silicate ions can have significant effects on their metabolism, activating genetic pathways, which can subsequently accelerate the recovery of damaged tissues. [4–7] For instance, calcium plays a central role in wound healing as it is involved in various cellular processes triggered by cutaneous injuries. [8, 9] In addition, internalised calcium is known to regulate inflammatory cell infiltration and favour the proliferation of fibroblasts. [10, 11] Few examples are available in the literature, demonstrating that a biomaterial-based approach is a viable strategy for the local delivery of calcium in wounded skin. [12–15] Kawai *et al.* developed calcium-based nanoparticles from a fetal bovine serum that can readily disintegrate in acidic pH, delivering ionised calcium. Intravenous injection in female Balb/cmice revealed a significant increase in the resorption of the wound as compared to the control. [15]

In the wider context of soft tissue regeneration, bioactive ceramics and glasses can deliver ions that have therapeutic properties. [3, 16] Ionic chemical cues can be present within the structure of the inorganic construct either as network modifier/former for bioactive glasses or as a part of the crystal lattice for bioceramics and can be

released upon hydrolytic degradation when immersed in body fluid. [17] However, most of the engineered bioactive glasses and ceramics have been designed towards the regeneration of hard tissue. Thus, the release of these active ions often comes with a great variation in surface chemistry, favouring the surface nucleation of bone-like crystal, an essential step in the osteoconduction cascade. [18]

While this is considered to be a desirable point in the regeneration of hard tissues, it may be a source of complications in regeneration of soft-tissues as it can lead to calcification, in particular for cardiovascular tissues. [19] In this report, we present a proof-of-concept for the fabrication of open 3D composite templates, allowing the release of inorganic chemical cues from bioactive glasses or ceramics while inhibiting the formation a hydroxyapatite layer on the surface of the template. A coaxial electrospinning setup was used to create a polymeric core-shell non-woven fabric within which the inorganic particles were loaded in the core of the fibres protected by a polymeric shell. [20] One important criterion of this engineered system is that the shell layer must uptake water from the surrounding body fluid in order to trigger the hydrolytic degradation of the inorganic particles and subsequent diffusion of the therapeutic ions in the media.

In order to validate this proof of concept, we selected silicon-containing vaterite (SiV) as an inorganic phase. SiVs are non-thermodynamically stable calcium carbonate spherical particles of approximately 1 μm which can release calcium and organo-silicate ions upon immersion in aqueous media. [21–24] When directly exposed to aqueous media, full conversion into calcite is observed within 1 h with a dissolution rate tailorable as a function of the synthesis parameters. Poly(lactic acid) was selected as an organic phase for the core of the fibers since this composite has already been

successfully electrospun. [25–28] Poly(D,L-lactide-*co*-glycolide) (PDLLG) was selected as an outer layer for its ability to uptake water and therefore allowing the hydrolytic degradation of the enclosed SiV particles. [20, 29, 30] The effect of the relative diameter of the inner core to the size of the PDLLG shell on the mechanical properties, dissolution behaviour, and apatite nucleation was investigated.

2 Experimental section

2.1 Materials

Poly(L-lactic acid) (PLLA, Mitsui Chemicals, Co., Ltd. Japan; M_w = 140 kDa), poly(D,L-lactide-*co*-glycolide) (PDLLG, Purasorb® PDLLG, Purac Biomaterials) and siloxane-containing vaterite (SiV, Yabashi Industries, Co., Ltd. Japan, 2.6 wt% of silicon, 1.4 μm in diameter) were used as received. All other chemicals were purchased from Wako Pure Chemical Industries, Japan.

2.2 Preparation of core-shell composite fibers by coaxial electrospinning

SiVPC (SiV/PLLA composite) was prepared by a melt-kneading method. [25] PLLA was poured into a preheated kneader and stirred for 5 min at 200 ^{o}C, and then mixed with SiV and stirred for another 10 min. The mass ratio of SiV to PLLA was set to 60 wt%. Coaxial electrospinning equipment (Kato Tech, NEU, Japan) was used to prepare the core-shell composite fibers. SiVPC (10 wt%) and PDLLG (15 wt%) were separately dissolved in chloroform and stirred at room temperature for 12 h. Each solution was loaded into separate syringes and set up on a pump (FP-W-100, Melquest,

Toyama, Japan). The syringes were connected to the coaxial needles (inner diameter Φ_{in} = 0.50 mm, outer diameter Φ_{out} = 1.10 mm) to form a concentric nozzle, with PDLLG and SiVPC representing the shell and the core of the electrospun fibers, respectively. The drum collector, with a tangential velocity of 2 m·min^{-1} wrapped in aluminum foil, was placed at 150–200 mm from the nozzle. The electrospinning was carried out applying a of +12 kV potential between the nozzle and the collector for 4 h, at room temperature with a relative humidity of ≈ 50 %. A schematic of the setup is shown in Figure 4–1.

The extrusion rate of the SiVPC shell was set to 63 mL·min^{-1}. The extrusion rate of the core layer (SiVPC) was set relatively to the shell at 2 × (CS-1) and 10 × (CS-2) slower. Conventional fibers were also prepared using the above method and a single needle from SiVPC and pure PDLLG dissolved in chloroform at 13 wt% and 15 wt%, respectively.

2.3 Characterisation of core-shell composite fibers

Morphologies of the surfaces and the fracture surfaces of the fibers were observed with a scanning electron microscope (SEM, JSM-6301F, JEOL, Japan) after coating with amorphous osmium. The diameters of core-shell fibers were measured from 40 randomly chosen fibers using Image J software. The cross sections were observed by soaking the fibers in liquid nitrogen for 2 min and breaking with tweezers. Tensile test was conducted on an Autograph (AGS-G, Shimadzu, Japan). The experiment followed the Japanese Industrial Standard JIS L1015. All samples were cut using a metal punch (50 mm × 10 mm). The grip-to-grip distance was 40 mm and the

samples were elongated at a constant tensile rate of 1 mm·min $^{-1}$ until failure. Each composition was run in triplicate.

2.4 Ion release behavior

The ion release behavior of the fibers was evaluated as previously described [23] in TBS. Briefly, 1000 mL of TBS was prepared by dissolving 6.118 g of tris(hydroxymethyl) aminomethane in distilled water at 36.5 ^{o}C, then adjusting pH to 7.4 with 1 M hydrochloric acid. 20 mg of sample was placed in polypropylene containers, subsequently filled with 10 mL, tightly sealed, and kept in an incubation oven at 36.5 ^{o}C in static state. At each time point (3 h, 6 h, 12 h, 3 d, 7 d and 10 d), samples were taken out from the solution, rinsed with DW and dried overnight. The concentrations of silica and calcium ions in the residual solutions were measured by inductively coupled plasma atomic emission spectroscopy (ICP-AES; ICPS-7000, Shimadzu, Japan). The ICP-AES was calibrated prior to use using calcium and silicon standard solutions at 2, 10, 40 mg·mL^{-1}. Each time point was run in triplicate for statistical relevance.

2.5 Apatite-forming ability

Simulated body fluid (SBF, pH = 7.4) [31] consisting of 142.0 mM Na^{+}, 5.0 mM K^{+}, 1.5 mM Mg^{2+}, 2.5 mM Ca^{2+}, 148.3 mM Cl^{-}, 4.2 mM HCO^{3-}, 1.0 mM HPO_4^{2-}, 0.5 mM SO_4^{2-} was prepared by dissolving reagent grade NaCl, $NaHCO_3$, KCl, $K_2HPO_4 \cdot 3H_2O$, $MgCl_2 \cdot 6H_2O$, HCl, $CaCl_2$, and Na_2SO_4 in distilled water at 36.5 ^{o}C, and then using tris(hydroxymethyl) aminomethane and 1 M hydrochloric acid to adjust

pH to 7.4. 20 mg of samples was immersed in10 mL of SBF and kept at 37 ^{o}C in static state for 1 or 3 days. Samples were then washed with distilled water and dried in air.

For characterization of the crystalline phases, an X-ray diffraction (XRD, X'pert X-ray Diffractometer, Philips) analysis was conducted (Cu*Ka* , 50 kV, 40mA). The scan rate was 0.01 ^{o}·s $^{-1}$ and a 2θ range was from 20 ^{o} to 60 ^{o}. Before tests, the dried sample were cut to 10 mm $\times$ 20 mm.

3 Results and discussion

3.1 Preparation of the core-shell composite fibers varying the shell wall thickness

Figure 4–1 shows the experimental setup used to obtain non-woven core-shell fibers composed of SiV particles embedded in poly(L-lactic acid) for the inner fiber and poly(D,L-lactide$_{75}$-*co*-glycolide$_{25}$) for the shell. Coaxial-electrospinning consists of applying a high-voltage to concentric needles from which two solutions of different compositions were fed. The variables affecting the coaxial-electrospinning were conceptually similar to those of single jet. [32] However, key parameters had to be carefully selected in order to achieve an uniform coating of the sheath polymer onto the core fibres, which can be found in Table 4–1: [33] (i) the working range of applied voltage used was found to be between 12 to 16 kV, guaranteeing the formation of a single Taylor cone comprising both the core and the shell as shown the inset of Figure 4–1. Moghe *et al.* described that a subcritical voltage could lead to a single jet of sheath polymer, whereas a supercritical voltage could lead to multiple jets, spinning separately the core and the shell. [33] However, this phenomenon was not observed here. (ii) The

stabilization of the Taylor cone was obtained due to the low interfacial tension between the core and shell solutions as chloroform was used as solvent for both solutions, which also favored the formation of uniform core-shell fibers. [34] (iii) Intermixing of the core and shell solutions was avoided by assuring that the difference in viscosity between two liquids was sufficient and that the flow rate of the core solution was at least twice lower than the sheath solution. [35] (iv) Finally, the flow rate of the core solution must be high enough in order to facilitate the formation of an inner jet and uniform fibers without beading. [36] Here, a fixed flow rate of 63 $mL \cdot min^{-1}$ was selected for the shell solution, while varying flow rate from 6.8 (CS-2) to 26.4 (CS-1) $mL \cdot min^{-1}$, expecting an increase of the inner diameter and overall fiber diameters as an increase of the core solution flow rates. [33, 36, 37]

Figure 4–2 shows SEM pictures of the fibers and their cross-sections after the electrospinning process, from which the characteristic sizes of the cores and shells were extracted and summarised in Table 4–1. Uniform fibers were produced with no apparent disruption of the core relative to the shell. Cross-sectioning of the fibers revealed that the SiV particles were well confined within the core of the fibers, suggesting that no inter-mixing of the solution occurred during the electrospinning process. Interestingly, the overall diameter of the fibers, of an approximate value of 10 μm, did not vary by decreasing the flow rate of the core solution, as suggested elsewhere in the literature. [36–38] Instead, the core diameter decreased from 7.4 μm at 26.4 $\mu L \cdot min^{-1}$ to 5.4 μm at 6.8 $\mu L \cdot min^{-1}$. Conventionally the viscosity of the sheath solution is set higher than the core to facilitate the formation of a uniform Taylor cone, counterbalancing the interfacial tension. [34, 36, 39] However, due to the composite nature of the core solution, this criterion could not be validated here, which nonetheless did not have

detrimental impact on electrospinnability of the material. Thus, we hypothesized that when the differential viscosity between the sheath and core solution is inverted, the rapid drying of the sheath solution relative to the core induced a sudden increase of the interfacial tension between the two liquids, and as a result stress hardened the core fibers during the whipping process. The direct consequence was that the core diameter could be controlled by its flow rate. In order to validate our observation, the experiment was replicated with a core solution flow rate 20 times lower than the sheath solution. Fibres with an overall diameter of 11 ± 2 μm and an inner diameter of 4.2 ± 1 μm were obtained (shows in supplementary Figure 4–S1), confirming the observation made above. The morphology of the fibers were also characterized by SEM as shown in Figure 4–2. Fibres exhibited rough surfaces, with potential porosity, regardless of the experimental condition used. Several reports on single jet electrospinning demonstrated that the surface morphology of fibers made from polyester is dictated by complex interactions between the polymer, solvent and the local environment in which process is conducted. [40, 41] Here, experiments were conducted at room temperature with a relative humidity of 50 % and the morphology of the fibers were in good agreement with the these obtained by Putti *et al.* using poly(ε-caprolactone) in $CHCl_3$, under the same conditions. [40]

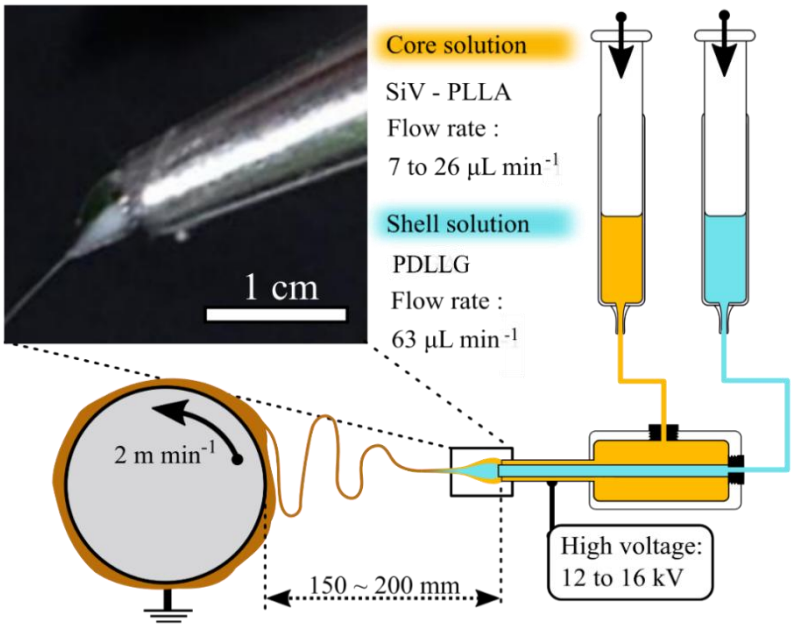

Fig. 4–1. Schematic representing the coaxial electrospinning setup used here to produce core-shell fibers with a photograph of the concentric spinneret (inset).

Table 4–1. Summary of the electrospinning parameters used to fabricate the core-shell composite fibers and their characteristic sizes.

Entry	Ratio [a] LA/GA	Viscosity [b] ($Pa{\cdot}s^{-1}$)	Polymer content [c] (wt%)	Feed rate [d] ratio	Voltage [e] (kV)	Fiber Φ [f] (µm)	Wall thickness [f] (µm)
SiVPC	100/0	4600	10	—	12	10 ± 1	—
CS-1	75/25	2.1	15	2.4	12	10 ± 2	1.3 ± 0.7
CS-2	75/25	2.1	15	9.2	12	10 ± 2	2.3 ± 0.1
CS-3	85/15	2.5	15	2.4	15	12 ± 2	1.6 ± 0.1
CS-4	50/50	2.2	13	2.4	16	11 ± 3	1.3 ± 0.6

[a] Molar ratio of lactic and glycolic acid in poly(D,L-lactide-*co*-glycolide); [b] obtained from the polymer/polymer-composites solubilised in $CHCl_3$ as shown in [] [c]; [d] sheath to core flow rate ratio with a shell set at 63 $\mu L{\cdot}min^{-1}$; [e] voltage applied between the coaxial needle and the collector; [f] measured from the SEM micrograph $n = 40$.

3.2 Effect of the PDLLG wall thickness on ion release

In order to evaluate the ion release from the fibermats, 20 mg of SiVPC, CS-1 and CS-2 were immersed in 50 mM TBS with pH adjusted to 7.4. The silicon and calcium release profiles are shown in Figure 4–3a and were obtained by analyzing the collected solution by ICP-AES. Calcium and soluble silica from SiVPC burst in solution with initial release rates of $R_{SiVPC,Ca}$ = 27 μg·mL^{-1} h^{-1} and $R_{SiVPC,Si}$ = 8 μg·mL^{-1} h^{-1} reaching 314.5 ± 0.6 μg·mL^{-1} and 32.0 ± 0.8 μg·mL^{-1} after 1 d of immersion and 345.4 ± 5.1 μg·mL^{-1} and 32.3 ± 0.8 μg·mL^{-1} at 3 d for calcium and silicon, respectively, and staying constant thereafter. Both ions were released in media due to hydrolytic instability of the silicon-containing vaterite particles embedded within the PLLA matrix, with profile releases in agreement with our previous report. [22, 26, 28] The initial release rate of the calcium was only 3.4 times higher than silicon when silicon only represents 2.8% of the weight of the SiV particles. This means that the silicon release was relatively higher than calcium, which can be explained by the structural role that hydrolyzed 3-aminopropyltriethoxysilane (APTES), the silicon source in SiV, plays in SiV particles. [23] APTES stabilizes the premature crystalline phases during the synthesis of SiV particles by enclosing them in a peripheral layer. Thus, upon immersion of the particles in aqueous media, oligomeric and monomeric aminopropylsilanetriols were first released in solution, in a burst fashion, subsequently followed by the release of calcium. [23]

With the presence of a poly(D,L-lactide$_{75}$-*co*-glycolide$_{15}$) shell layer onto the SiVPC fibers, both initial rate of release and total amount released at 10 days were reduced with a more pronounced effect as the wall thickness increased. For instance, the calcium initial rate of release decreased to $R_{CS-1,Ca}$ = 16 μg·mL^{-1} h^{-1} and to $R_{CS-2,Ca}$ = 2

μg·mL^{-1} h^{-1} with a wall thickness of 1.3 and 2.3 μm, respectively. The hydrolytic degradation of the embedded SiV particles, through the PDLLG layer, was possible due to the water uptake of the shell layer. [30, 42]

However, despite the apparent reduction in concentration in calcium and silica with the increase of the wall thickness, it is difficult to draw firm conclusion as an increase in wall thickness came with a decrease in SiV particle content at a fixed mass of fibers. Thus, to alleviate the uncertainty, the total content in silica and calcium per gram of fibers was evaluated after alkaline digestion, allowing the normalization of the release profiles presented in Figure 4–3a, as shown in Figure 4–3b. This revealed that with an outer layer of 1.3 μm (CS-1), the general release rate of silica and calcium was reduced compared to SiVPC, however, with no statistical decrease of the initial rate. For instance, calcium was initially released at 7.0 ± 1 %·h^{-1} for SiVPC and 6.0 ± 1 %·h^{-1} for CS-1. With an outer thickness of 2.3 μm, the initial release rate was 2.5 ± 0.5, approximately half of SiVPC. In addition, it appeared that the modal release for CS-2 varied from CS-1 with a sustain release of calcium after 3 d immersion at a rate of release of 3 % d^{-1}. In order to verify whether this change in release behavior was due to a change in mechanism of release or just a consequence of the increase in shell thickness, the profiles in Figure 4–3b were fitted with the Weibull model, characterizing a purely diffusive, or Fickian, ionic transport, using the following equation: [43, 44]

$$\frac{M_t}{M_\infty} = 1 - \exp\left(-a \times t^b\right) \qquad (1)$$

where M_∞ is the total amount of released ions at infinity, M_t the amount of ions released at t, a and b constants. All release profiles from the core-shell fibers could be fitted with the Weibull model with a R^2 above 0.99, suggesting that the ionic release from the SiV

particles through the PDLLG layer was purely diffusive. In addition, when using PDLLG75 as a template, the value taken by *b* could inform on the mechanism of diffusional release and the degree of disordering of the medium (*i.e.* the PDLLG shell). [45, 46] Since the same polymer was used as a shell for CS-1 and CS-2, *b* is only describing the change in release mechanism. Thus, with CS-2 ($b = 0.354 \pm 0.01$) the diffusion was characteristic of a percolation cluster whereas with CS-1 ($b = 0.954 \pm 0.05$) the diffusion followed a first order with regards to the Fick's law of diffusion, highlighting changes in release mechanism with the wall-thickness. In addition, this model suggests that increasing or decreasing the ordering of the template could also lead to variations in the ionic release profiles. Fortunately, the degree of ordering in PDLLG and its ability to uptake water can be tuned as a function its chemical composition, by varying the relative content of lactic to glycolic residue in the copolymer. An increase in lactic content would lead in a more hydrophobic shell and vice versa. To verify the validity of this hypothesis, the core-shell fibres similar to CS-1 in geometry were produced using PDLLG with a lactic to glycolic molar ratio of 85 : 15 (CS-3) and 50 : 50 (CS-4) (SEM pictures available in ESI, Figure 4–S2) and immersed in TBS as shown in Figure 4–4 (silicon release in Figure 4–S3). CS-1 and SiVPC were plotted as a control. As expected the release behavior of PDLLG (85 : 15) was slower than PDLLG (75 : 25), which was itself higher than PDLLG (50 : 50). The data were fitted with the Weibull model and showing an increase in the value *b* with PDLLG (50 : 50) to 1.515 and a decrease with PDLLG (85 : 15) to 0.724, indicating variations in the mechanism of release. [46] This highlights the complexity of ionic diffusion through PDLLG membranes or shell but also shows the high degree of tailor -ability of the system. It is important to note that these release profiles could also be greatly influenced

with the hydrolytic stability of the inorganic construct embedded with the core of the fibers and are only valid for SiV particles.

3.3 Apatite-forming ability

The precipitation of hydroxyapatite onto the surface of glasses or ceramics is known to be a surface nucleation driven process, where topography, surface chemistry and local environment play detrimental roles in the mechanism. [18] By enclosing the SiVPC fibers with a bio-inert polymer, we hypothesized that crystal nucleation could be suppressed. [47] To confirm this statement, SiVPC, CS-1 and CS-2 were immersed in simulated body fluid (SBF) over 3 d and the variation in surface chemistry was monitored by XRD and SEM. This measurement is not to be related to the potential *in vivo* performance of these non-woven fibers but to understand the change in chemistry upon immersion in media that have the same ionic strength that blood plasma. [48]

Figure 4–5 shows the SEM micrographs of the fibermats before and after 1 and 3 d of immersion in SBF. After 1 d, cauliflower-like crystals of ≈ 1 μm were partially covering the SiVPC fibers, which slightly grew in size and number after 3 d of immersion. The morphology of the crystals was typical of early stage nucleation of calcium-phosphate on bioactive materials. [18] It is likely that the rapid increase in calcium concentration along with the rough surface of the fibers could have favored the nucleation of calcium-phosphate crystal as SBF is supersaturated towards hydroxyapatite. [49] However, it is unclear whether the polymer or the exposed SiV particles acted as nucleation center. The presence of a shell layer significantly reduced or suppressed the crystal nucleation on the surface of the fibers. Upon immersion of CS-1, submicron particles could be observed on the surface of the fibers. However, it is

difficult to appreciate whether these particles were formed by nucleation, or were SiV particles exposed by early erosion of the PDLLG shell layer. With a wall thickness of 2.3 μm, such as with CS-2, no precipitate could be observed, with smooth fibers at 1 and 3 d of immersion, result of the shell hydration. [30, 42] Figure 4–6 shows the XRD patterns before and after immersion in SBF for SiVPC, CS-1 and CS-2. SiV particles are characterized by diffraction peaks at 21^{o} and 25^{o} and 33^{o} 2θ (ICSD 18127), originating from the (004), (110) and (114) planes of their hexagonal unit cell, respectively. [23] Before immersion, the intensity of diffracted peaks, corresponding to SiV, decreased with an increase of the wall thickness. Clear diffraction at peak at $2\theta \approx 32^{o}$ could be observed after 3 d of immersion for SiVPC, which is characteristic of crystallized calcium-phosphate (ICSD 01-084-1998) and corroborated the observations made with SEM. However, the definition of the peak was not sufficient to conclude with certainty that the crystal formed was hydroxyapatite. With CS-1, vaterite was the only crystalline phase detected, regardless of the immersion period whereas calcite was detected after 1 d of immersion for CS-2 (ICSD 52151). It is likely that with CS-2 the slow ionic diffusion along with the efficient hydration of the shell led to the conversion of SiV into calcite within the core of the fibers as no crystal could be seen on their surface.

3.4 Mechanical properties of the core-shell composite fibers

It is important that when synthesizing synthetic materials for medical application, the resulting template has enough strength to be physically handled and manipulated by the surgeons without breaking. [2] SiVPC is known to be brittle due to the high loading of inorganic particles (60 wt%). [26] Thus, additionally to the above proof of concept,

we investigated whether the addition of a PDLLG shell layer could have a beneficial effect onto the mechanical properties of the electrospun composites.

Tensile test was performed SiVPC, CS-1, CS-2 and the resulting stress-strain curves are shown in Figure 4–7 and the extracted tensile strength, elongation at break and Young's modulus in Table 4–2. As expected, SiVPC fibermat was brittle with an elongation at break of 1.77 ± 0.79 %. Upon the addition of a PDLLG shell layer, the mode of deformation went from brittle to ductile, with a proportional increase of the mechanical properties with the increase of the wall thickness. For instance, the Young's modulus of the fibermats, extracted for the elastic region, went from 22 MPa for SiVPC to 118 for CS-2 along with 530 % increase in the tensile strength and 1441 % in elongation at break.

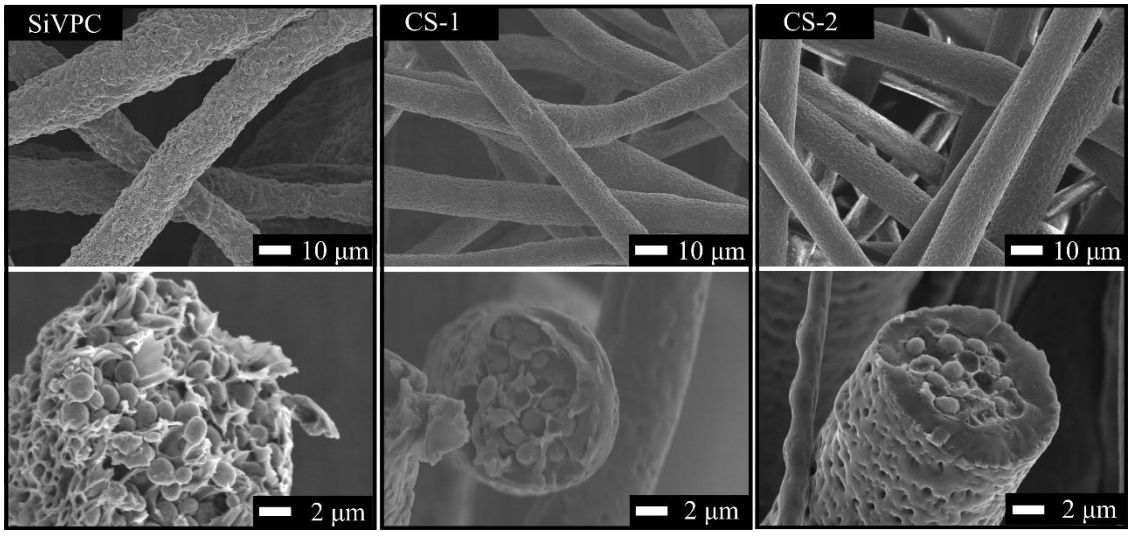

Fig. 4–2. SEM micrographs showing the porous structure of the core-shell fibers after electrospinning and their corresponding cross-section.

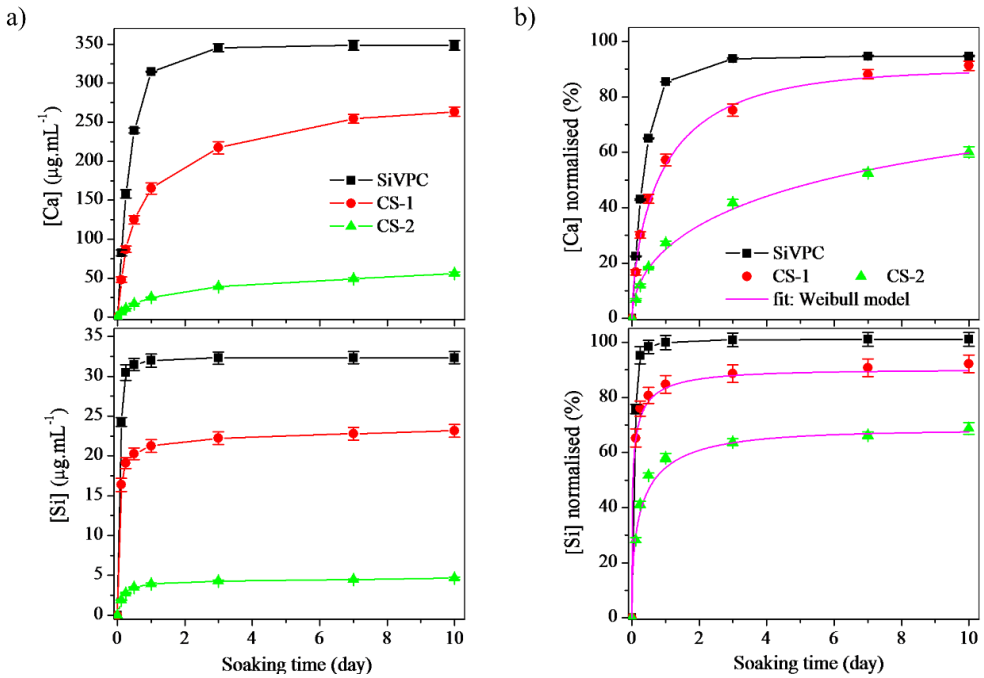

Fig. 4–3. Calcium and silicon release profiles upon immersion in TBS over 10 d with (a) the concentration given in mg·mL^{-1} and (b) the normalized concentration. The normalized profiles of the core-shell fibers were fitted using eqn (1).

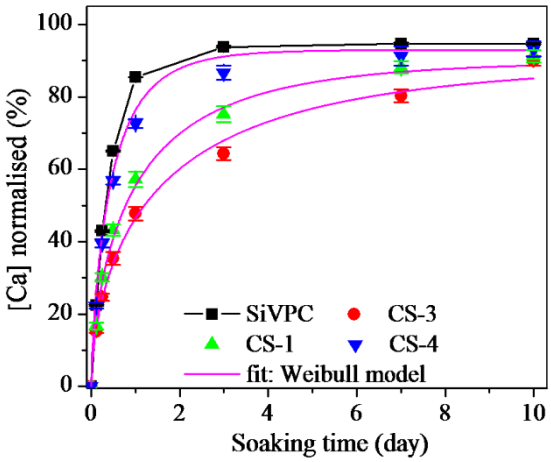

Fig. 4–4. Normalised calcium release profiles in TBS from core-shell fibers of the same wall-thickness, varying the ratio of lactic to glycolic acid in the PDLLG shell layer. The normalized profiles of the core-shell fibers were fitted using eqn (1).

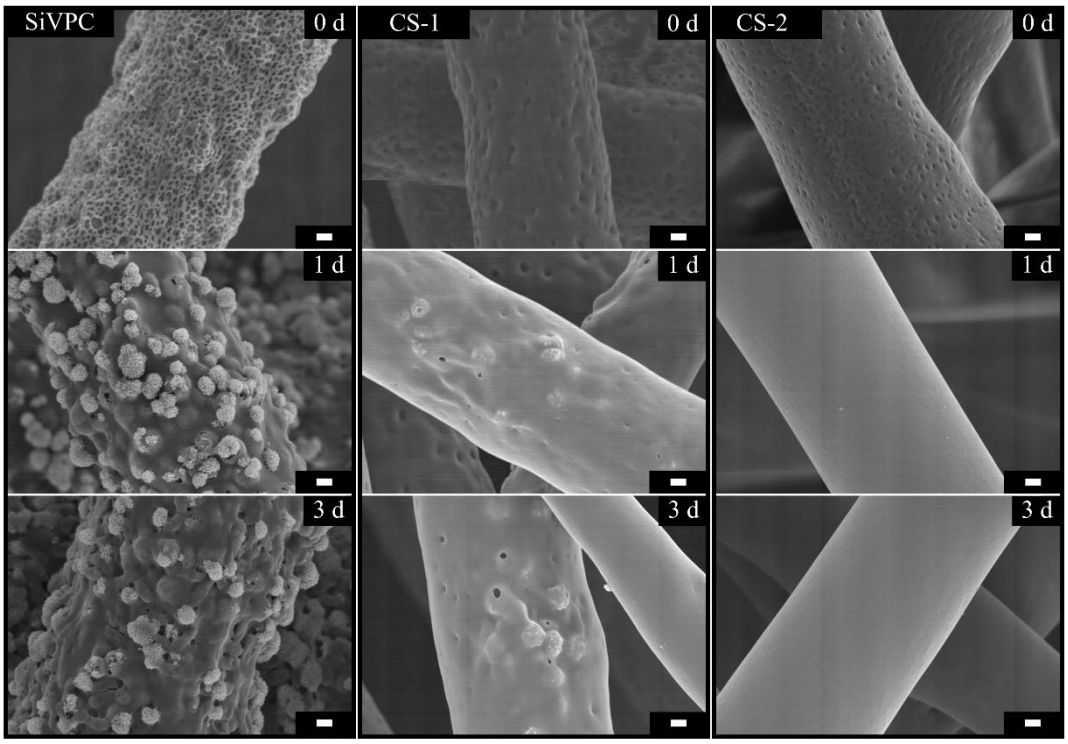

Fig. 4–5. SEM micrographs of SiVPC, CS-1 and CS-2 before and after immersed in SBF for 1 day and 3 days, the scale bar is 1 μm.

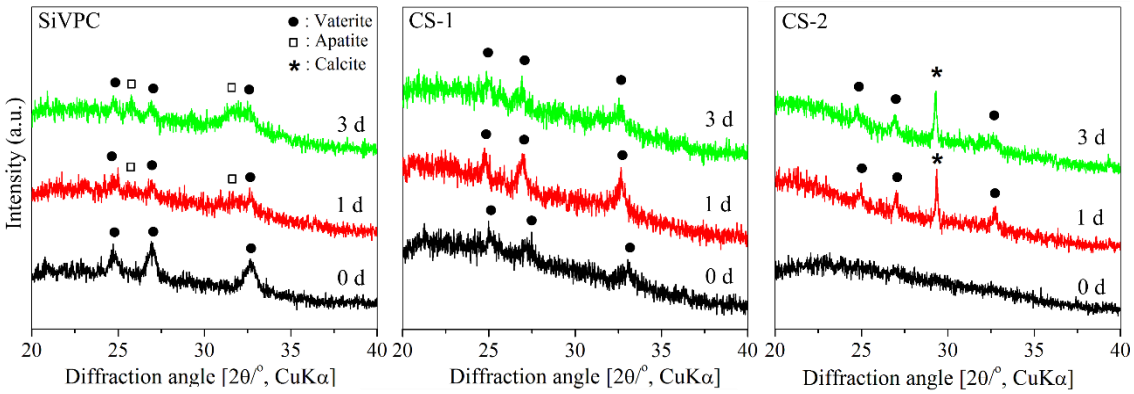

Fig. 4–6. XRD patterns of the core-shell fibers before and after 1 d and 3 d of immersion in simulated body fluid.

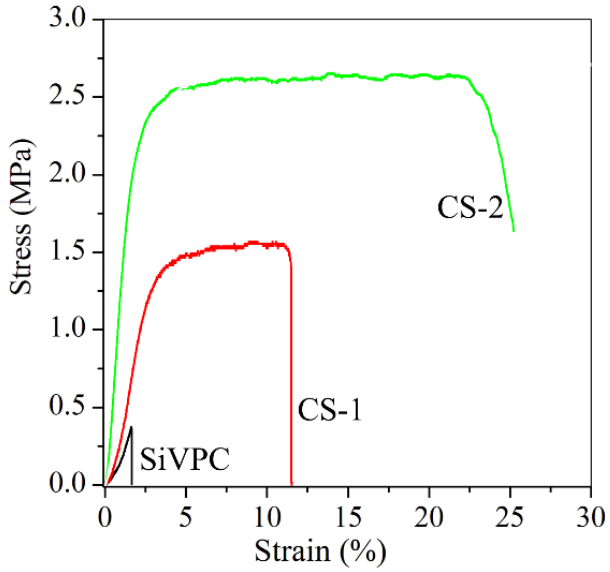

Fig. 4–7. Typical stress-strain curves obtained from tensile deformation of the fibremats.

Table 4–2. Summary of values extracted from the stress-strain curve in Figure 4–7 describing the mechanical properties of the core-shell fibers. Values are given from a population of $n = 3$.

Samples	Tensile strength [MPa]	Elongation at break [%]	Young's modulus [MPa]
SiVPC	0.52 ± 0.33	1.77 ± 0.79	22 ± 1
CS-1	1.78 ± 0.39	10.60 ± 0.80	49 ± 1
CS-2	2.76 ± 0.33	25.52 ± 7.89	118 ± 11

4 Conclusions

- SiV/PDLLG core-shell composite fibers were prepared by coaxial electrospinning, the core consisted of a hybrid between siloxane-containing vaterite and PLLA while the shell consisted of PDLLG.
- By variety of the wall-thickness, the apatite-forming ability of bioactive inorganic construct could be suppressed while retaining the release of inorganic chemical cues in the surrounding media.
- This engineered strategy could opened new perspectives to the large library of inorganic construct that have been originally designed for the repair of hard tissue towards the regeneration of soft tissue, where calcification could lead to non-negligible complications.
- These non-woven porous materials could also be used as investigation platform to study the effect of local ionic release onto the surrounding cell metabolism.

References

[1] V. Miguez-Pacheco, L. L. Hench, A. R. Boccaccini, Bioactive glasses beyond bone and teeth: emerging applications in contact with soft tissues. *Acta Biomater.*, **13**, 1-15 (2015).

[2] J. R. Jones, Review of bioactive glass: From Hench to hybrids. *Acta Biomater.*, **9**, 4457-4486, (2013).

[3] M. N. Rahaman, D. E. Day, B. S. Bal, Q. Fu, S. B. Jung, L. F. Bonewald, A. P. Tomsia, Bioactive glass in tissue engineering. *Acta Biomater.*, **7**, 2355-2373 (2011).

[4] A. Hoppe, N. S. Goldal, A. R. Boccaccini, A review of the biological response to ionic dissolution products from bioactive glasses and glass-ceramics. *Biomaterials*, **32**, 2757-2774 (2011).

[5] A. L. B. Ma ɋn, M. Jacquemin, S. J. Page, S. Li, S. Bertazzo, M. M. Stevens, J. V. Hanna, J. R. Jones, Lithium-silicate sol-gel bioactive glass and the effect of lithium precursor on structure-property relationships. *J. Sol-Gel Sci.Technol.*, **81**, 84-94, (2016).

[6] A. Obata, Y. Takahashi, T. Miyajima, K. Ueda, T. Narushima and T. Kasuga, Effects of niobium ions released from calcium phosphate invert glasses containing Nb_2O_5 on osteoblast-like cell functions. *ACS Appl. Mater. Interfaces*, **4**, 5684-5690 (2012).

[7] G. Poologasundarampillai, D. Wang, S. Li, J. Nakamura, R. Bradley, P. Lee, M. Stevens, D. McPhail, T. Kasuga, J. Jones, Cotton-wool-like bioactive glasses for bone regeneration. *Acta Biomater.*, **10**, 3733-3746 (2014).

[8] S. K. Yoo, C. M. Freisinger, D. C. LeBert, A. Huttenlocher, Early redox, Src family kinase, and calcium signaling integrate wound responses and tissue regeneration in zebrafish. *J. Cell Biol.*, **199**, 225-234 (2012).

[9] J. V. Cordeiro, A. Jacinto, The role of transcription-independent damage signals in the initiation of epithelial wound healing. *Nat. Rev. Mol. Cell Biol.*, **14**, 249-262 (2013).

[10] A. Jadali, S. Ghazizadeh, Protein kinase D is implicated in the reversible commitment to differentiation in primary cultures of mouse keratinocytes. *J. Biol. Chem.*, **285**, 23387- 23397 (2010).

[11] D. D. Bikle, D. Ng, C.-L. Tu, Y. Oda, Z. Xie, Calcium- and vitamin D-regulated keratinocyte differentiation. *Mol. Cell. Endocrinol.*, **177**, 161-171 (2001).

[12] Y. Suzuki, Y. Nishimura, M. Tanihara, K. Suzuki, T. Nakamura, Y. Shimizu, Y. Yamawaki, Y. Kakimaru, Evaluation of a novel alginate gel dressing: cytotoxicity to fibroblasts in vitro and foreign-body reaction in pig skin in vivo. *J. Biomed. Mater. Res., Part A*, **39**, 317-322 (1998).

[13] J. W. Doyle, T. P. Roth, R. M. Smith, Y. Q. Li, R. M. Dunn, Effect of calcium alginate on cellular wound healing processes modeled *in vitro*. *J. Biomed. Mater. Res.*, **32**, 561-568 (1996).

[14] J. S. Boateng, K. H. Matthews, H. N. Stevens, G. M. Eccleston, Wound healing dressings and drug delivery systems: a review. *J. Pharm. Sci.*, **97**, 2892-2923 (2008).

[15] K. Kawai, B. J. Larson, H. Ishise, A. L. Carre, S. Nishimoto, M. Longaker, H. P. Lorenz, Calcium-based nanoparticles accelerate skin wound healing. *PLoS One*, **6**, e27106 (2011).

[16] A. El-Ghannam, Bone reconstruction: from bioceramics to tissue engineering. *Expert Rev. Med. Devices*, **2**, 87-101 (2005).

[17] T. Kasuga, Bioactive calcium pyrophosphate glasses and glass-ceramics. *Acta Biomater.*, **1**, 55-64 (2005).

[18] A. L. B. Maçon, T. B. Kim, E. M. Valliant, K. Goetschius, R. K. Brow, D. E. Day, A. Hoppe, A. R. Boccaccini, I. Y. Kim, C. Ohtsuki, T. Kokubo, A. Osaka, M. Vallet-Regi, D. Arcos, L. Fraile, A. J. Salinas, A. V. Teixeira, Y. Vueva, R. M. Almeida, M. Miola, C. Vitale-Brovarone, E. Verne, W. Holand, J. R. Jones, A unified in vitro evaluation for apatite-forming ability of bioactive glasses and their variants. *J. Mater. Sci.: Mater. Med.*, **26**, 115 (2015).

[19] W. Karwowski, B. Naumnik, M. Szczepanski, M. Mysliwiec, The mechanism of vascular calcification-a systematic review. *Med. Sci. Monit.*, **18**, 1-11 (2012).

[20] J. Wang, P. Zhou, A. Obata, J. R. Jones, T. Kasuga, Preparation of cotton-wool-like poly(lactic acid)-based composites consisting of core-shell-type fibers. *Materials*, **8**, 7979-7987 (2015).

[21] A. Obata, S. Tokuda, T. Kasuga, Enhanced in vitro cell activity on silicon-doped vaterite/poly(lactic acid) composites. *Acta Biomater.*, **5**, 57-62 (2009).

[22] J. Nakamura, T. Kasuga, Preparation of siloxane-containing vaterite particles with red-blood-cell-like morphologies and incorporation of calcium-salt polylactide for bone regenerative medicine. *J. Ceram. Soc. Jpn.*, **121**, 792-796 (2013).

[23] J. Nakamura, G. Poologasundarampillai, J. R. Jones, T. Kasuga, Tracking the formation of vaterite particles containing aminopropyl-functionalized silsesquioxane and their structure for bone regenerative medicine. *J. Mater. Chem. B*, **1**, 4446-4454 (2013).

[24] S. Yamada, Y. Ota, J. Nakamura, Y. Sakka, T. Kasuga, Preparation of siloxane-containing vaterite doped with magnesium. *J. Ceram. Soc. Jpn.*, **122**, 1010-1015 (2014).

[25] T. Wakita, J. Nakamura, Y. Ota, A. Obata, T. Kasuga, S. Ban, Effect of preparation route on the degradation behavior and ion releasability of siloxane-poly(lactic acid)-vaterite hybrid nonwoven fabrics for guided bone regeneration. *Dent. Mater. J.*, **30**, 232-238 (2011).

[26] K. Fujikura, S. Lin, J. Nakamura, A. Obata, T. Kasuga, Preparation of electrospun fiber mats using siloxane-containing vaterite and biodegradable polymer hybrids for bone regeneration. *J. Biomed. Mater. Res., Part B*, **101**, 1350-1358 (2013).

[27] A. Obata, T. Hotta, T. Wakita, Y. Ota, T. Kasuga, Electrospun microfiber meshes of silicon-doped vaterite/poly(lactic acid) hybrid for guided bone regeneration. *Acta Biomater.*, **6**, 1248-1257 (2010).

[28] T. Wakita, A. Obata, G. Poologasundarampillai, J. R. Jones, T. Kasuga, Preparation of electrospun siloxane-poly(lactic acid)-vaterite hybrid fibrous membranes for guided bone regeneration. *Compos. Sci. Technol.*, **70**, 1889-1893 (2010).

[29] J. K. Perron, H. E. Naguib, J. Daka, A. Chawla, R. Wilkins, A study on the effect of degradation media on the physical and mechanical properties of porous PLGA 85/15 scaffolds. *J. Biomed. Mater. Res., Part B*, **91**, 876-886 (2009).

[30] H. K. Makadia, S. J. Siegel, Poly lactic-*co*-glycolic acid (PLGA) as biodegradable controlled drug delivery carrier. *Polymers*, **3**, 1377-1397 (2011).

[31] T. Kokubo, H. Takadama, How useful is SBF in predicting in vivo bone bioactivity? *Biomaterials*, **27**, 2907-2915 (2006).

[32] J. M. Deitzel, J. Kleinmeyer, D. Harris, N. C. B. Tan, The effect of processing variables on the morphology of electrospun nanofibers and textiles. *Polymer*, 42, 261-272 (2001).

[33] A. K. Moghe, B. S. Gupta, Co−axial electrospinning for nanofiber structures: preparation and applications. *Polym. Rev.*, **48**, 353-377 (2008).

[34] J. H. Yu, S. V. Fridrikh, G. C. Rutledge, Production of submicrometer diameter fibers by two-fluid electrospinning. *Adv. Mater.*, **16**, 1562-1566 (2004).

[35] A. Townsend-Nicholson, S. N. Jayasinghe, Cell electrospinning: a unique biotechnique for encapsulating living organisms for generating active biological microthreads/scaffolds. *Biomacromolecules*, **7**, 3364-3369 (2006).

[36] M. Wang, J. H. Yu, D. L. Kaplan, G. C. Rutledge, Production of submicron diameter silk fibers under benign processing conditions by two-fluid electrospinning. *Macromolecules*, **39**, 1102-1107 (2006).

[37] H. Na, P. Chen, S. C. Wong, S. Hague, Q. Li, Fabrication of PVDF/PVA microtubules by coaxial electrospinning. *Polymer*, **53**, 2736-2743 (2012).

[38] Y. Z. Zhang, X. Wang, Y. Feng, J. Li, C. T. Lim, S. Ramakrishna, Coaxial electrospinning of (fluorescein isothiocyanate-conjugated bovine serum albumin)-encapsulated poly(ε-caprolactone) nanofibers for sustained release. *Biomacromolecules*, **7**, 1049-1057 (2006).

[39] F. Elahi, W. Lu, G. Guoping, F. Khan, Core-shell fibers for biomedical applications-a review. *J. Bioeng. Biomed. Sci.*, **3**, 1-14 (2013).

[40] M. Putti, M. Simonet, R. Solberg, G. W. Peters, Electrospinning poly(ε-caprolactone) under controlled environmental conditions: influence on fiber morphology and orientation. *Polymer*, **63**, 189-195 (2015).

[41] L. Huang, N.-N. Bui, S. S. Manickam, J. R. McCutcheon, Controlling electrospun nanofiber morphology and mechanical properties using humidity *J. Polym. Sci., Part B: Polym. Phys.*, **49**, 1734-1744 (2011).

[42] D. J. Hines, D. L. Kaplan, Poly (lactic-*co*-glycolic acid) controlled release systems: experimental and modeling insights. *Crit. Rev. Ther. Drug Carrier Syst.*, **30**, 257-276 (2013).

[43] W. Weibull, A statistical distribution function of wide applicability. *J. Appl. Mech.*, **13**, 293-297 (1951).

[44] K. Kosmidis, P. Argyrakis, P. Macheras, Fractal kinetics in drug release from finite fractal matrices. *J. Chem. Phys.*, **119**, 6373-6377 (2003).

[45] V. Papadopoulou, K. Kosmidis, M. Vlachou, P. Macheras, On the use of the Weibull function for the discernment of drug release mechanisms. *Int. J. Pharm.*, **309**, 44-50 (2006).

[46] S. Giovagnoli, P. Blasi, M. Ricci, A. Schoubben, L. Perioli, C. Rossi, Physicochemical characterization and release mechanism of a novel prednisone biodegradable microsphere formulation. *J. Pharm. Sci.*, **97**, 303-317 (2008).

[47] F. G. Torres, S. N. Nazhat, S. H. S. M. Fadzullah, V. Maquet, A. R. Boccaccini, Mechanical properties and bioactivity of porous PLGA/TiO_2 nanoparticle-filled composites for tissue engineering scaffolds. *Compos. Sci. Technol.*, **67**, 1139-1147 (2007).

[48] M. Bohner, J. Lemaitre, Can bioactivity be tested in vitro with SBF solution? *Biomaterials*, **30**, 2175-2179 (2009).

[49] A. Oyane, H. M. Kim, T. Furuya, T. Kokubo, T. Miyazaki, T. Nakamura, Preparation and assessment of revised simulated body fluids. *J. Biomed. Mater. Res., Part A*, **65**, 188-195 (2003).

Supplementary figures

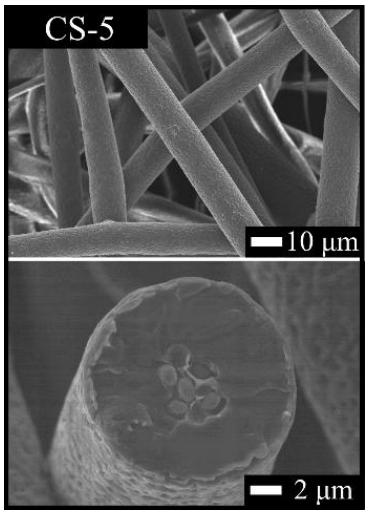

Fig. 4–S1. SEM micrographs of fibers and cross-sections morphologies of core-shell fibers with a relative extrusion speed between of the core to the shell of 20.

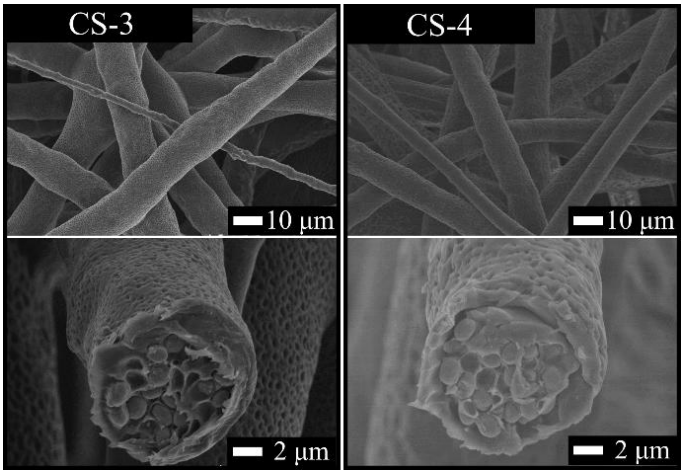

Fig. 4–S2. SEM micrographs of fibers and cross-sections morphologies CS-3 and CS-4.

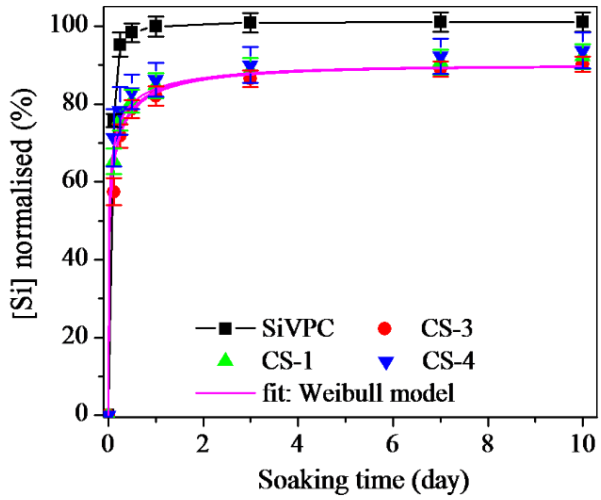

Fig. 4–S3. Normalised silicon ions release profiles from core-shell fibers of the same wall-thickness, varying the ratio of lactic to glycolic acid in the PDLLG shell layer. The normalized profiles of the core-shell fibres were fitted using eqn (1).

Chapter V Summary

In the present thesis, the objective is to prepare flexible biocomposite materials with inorganic materials and biodegradable polymer matrices. To design this biomaterials for tissue regeneration, it was of critical importance to apply therapeutically relevant aspects to stimulate cellar activity and angiogenesis. Therefore, SiV or SiV-derivative materials (MgSiV), which were with abilities to release therapeutic ions, and biodegradable polymer materials were used to fabricate bioactive composite materials. Ions-release behaviour, HA-forming ability, potential applications of SiV and MgSiV were investigated.

In chapter II, three kinds of composites containing MgSiV particles were prepared using PLLA, PDLLG75, and PDLLG50 as the polymeric matrices. The strong hydrophobicity of PLLA controlled the release of ions from the MgSiV-PLLA composite. The fast degradation of PDLLG50 induced a decrease in the pH of the TBS soaking solution. During a 7 d period, MgSiV-PDLLG75 composites exhibited continuous ion release and the pH of the soaking solution was found to be steady; these composites exhibited desirable water uptake ability and degradability, which helps to create pathways for ion release and diffusion.

In chapter III, PDLLG75 with ~2-μm-thick-layer was coated on a SiV/PLLA composite fiber by a coaxial electrospinning technique to meet the demands of filling various irregularly shaped bone voids. The obtained cotton-wool-like material was core-shell-structure and the fibres with a diameter of ~12 μm. In TBS, the initial burst release of calcium and silicate ions was effectively controlled. The mechanical flexibility of the composites material was drastically improved by the thin PDLLG75 coating, showed a ~60% recovery after removing the compressive load.

In chapter IV, a coaxial electrospinning process was applied to generate core-shell fibres by enclosing SiV/PLLA composite fiber within PDLLG shell. The results demonstrated a dramatic increase of mechanical flexibilities for the fibermats. The apatite-forming ability of the inorganic biomaterial (SiV) could be suppressed while retaining the release of inorganic ions in the surrounding media by modulating the thickness of PDLLG layer. This engineered strategy could open new perspectives to the large library of inorganic construct that have been originally designed for the repair of hard tissue towards the regeneration of soft tissue.

Publications including studies in this thesis

1) Preparation of cotton-wool-like poly(lactic acid)-based composites consisting of core-shell-type fibers

   Jian Wang, **Pin Zhou**, Akiko Obata, Julian R. Jones, Toshihiro Kasuga

   Materials, **8**, 7979-7987 (2015).

   DOI 10.3390/ma8115434

……Chapter III

2) Tailoring the delivery of therapeutic ions from bioactive scaffolds while inhibiting their apatite nucleation: a coaxial electrospinning strategy for soft tissue regeneration

   Pin Zhou, Jian Wang, Anthony L. B. Ma ̧on, Akiko Obata, Julian R. Jones, Toshihiro Kasuga

   RSC Advances, **7**, 3992-3999 (2017).

   DOI 10.1039/c6ra25645g

……Chapter IV

3) Dissolution behavior of Mg/Si-doped vaterite particles in biodegradable polymer composites

   Pin Zhou, Toshihiro Kasuga

   Express Polymer letters, **12**, 171-179 (2018).

   DOI org./10.3144/expresspolymlett.2018.15

……Chapter II

Acknowledgements

First of all, I want to express my sincere and deep appreciation to my supervisor Professor Toshihiro Kasuga for providing me the precious chance to study in his laboratory. His constant helping, valuable suggestions and unconditional supports throughout my Ph.D. studying period, which made my studying life in Nagoya Institute of Technology (NITech) valuable and rewarding. I would like to express my gratitude to Associate Professor Akiko Obata for valuable advices and comments on my research results. I would like to appreciate Associate Professor Hirotaka Maeda for warm help and kind advices. I am sincerely thankful to Dr. Anthony L. B. Maçon for helpful guidance and valuable advices. I would like to thank the supervisor of my Master course Professor Zhaobin Qiu for continuous assistance and support. I would like to show appreciate to Professor Feng Wang for providing me the precious chance to study in NITech as exchange student with Beijing University of Chemical Technology. I would like to thank Professor Shuli You for kind helping, meaningful advices and exciting discussions of various topics. I also would like to acknowledge all of members in Kasuga laboratory.

I want to take this chance to thank my fiance Dr. Yuanming Li and all my friends, especially to Mr. Kai Tian, Dr. Chen Guo, Miss Zinan Jiang, Dr. Tiphanie Maçon, Dr. Wai I Ho, Dr. Yutong Li, Dr. Maria Nelson, Dr. Chen Wang and Dr. Ce Tu.

At last, I would like to thank my parents for their unconditional supports and constant encouragements.

Pin Zhou